CEBAF PROPOSAL COVER SHEET

This Proposal must be mailed to:

CEBAF
Scientific Director's Office
12000 Jefferson Avenue
Newport News, VA 23606

A. TITLE: Measurement Of The Electric And Magnetic Elastic Structure Functions Of The Deuteron At Large Momentum Transfers

B. CONTACT PERSON: Gerassimos G. Petratos

ADDRESS, PHONE, AND ELECTRONIC MAIL ADDRESS:

SLAC, M/S 20
P.O. Box 4349
Stanford University
Stanford, CA 94309

415/926-4361
GGP@SLACVM

C. IS THIS PROPOSAL BASED ON A PREVIOUSLY SUBMITTED LETTER OF INTENT?

[ ] YES [XX] NO

IF YES, TITLE OF PREVIOUSLY SUBMITTED LETTER OF INTENT:

****

(CEBAF USE ONLY)

Receipt Date 1 OCT 91

Log Number Assigned PR-91-026

By [redacted]

September 30, 1991

CEBAF Proposal

MEASUREMENT OF THE ELECTRIC AND MAGNETIC ELASTIC STRUCTURE FUNCTIONS OF THE DEUTERON AT LARGE MOMENTUM TRANSFERS

K. A. Aniol, D. J. Margaziotis
California State University, Los Angeles, CA 90032

J. Gomez, S. K. Nanda
CEBAF, Newport News, VA 23606

C. C. Chang, H. D. Holmgren, P. G. Roos
University of Maryland, College Park, MD 20742

G. G. Petratos
SLAC, Stanford, CA 94309[*]

S. E. Kuhn, Z. E. Meziani
Stanford University, Stanford, CA 94305

C. J. Martoff
Temple University, Philadelphia, PA 19122

Spokesperson: G. G. Petratos

---

* *SLAC is not sponsoring this initiative as an Institution, given its policy of only supporting research activities at SLAC. The participation of G. G. Petratos is possible because of his fixed term research appointment at SLAC.*

ABSTRACT

We propose two experiments to measure forward and 180° elastic electron-deuteron scattering to the highest momentum transfers possible, limited by a cross section sensitivity of about 2×10^{-42} cm^2/sr. Both measurements will detect the recoiling deuterons in coincidence and will require a high power liquid deuterium target. The results are expected to play an important role in understanding the short-range structure of the deuteron in terms of nucleonic, mesonic and quark degrees of freedom.

The forward angle experiment will extend our knowledge of the electric elastic structure function $A(Q^2)$ up to possibly Q^2= 6 (GeV/c)^2 and significantly improve the existing low Q^2 data. The measurements will use the Hall-A spectrometer facilities. The scattered electrons will be detected in the electron High Resolution Spectrometer and the recoiling deuterons in the hadron High Resolution Experiment. We request 25 days of data taking with 50% efficiency and 5 days of checkout time.

The backward angle experiment will extend our knowledge of the magnetic elastic structure function $B(Q^2)$ of the deuteron up to possibly Q^2= 5 (GeV/c)^2 and accurately map its diffraction minimum. This experiment can be performed either in Hall-A or in Hall-C. The scattered electrons will be detected in a 180° spectrometer system made up of surplus magnets. The recoil deuterons will be detected in coincidence in a 0° spectrometer consisting of a dipole magnet in addition to either the Hall-C High Momentum Spectrometer or the Hall-A hadron High Resolution Spectrometer. We request 75 days of data taking considering an overall efficiency of 40% and 15 days of checkout time.

1. MOTIVATION

Electron scattering from the deuteron has long been an extremely important means of understanding the properties of the nuclear two body system. The deuteron electromagnetic form-factors in particular, measured in elastic scattering, offer unique opportunities to test models of the short-range nucleon-nucleon interaction, meson-exchange currents and isobaric configurations as well as the possible influence of explicit quark degrees of freedom.

The cross section for elastic electron deuteron scattering is described by the Rosenbluth formula:

$$\frac{d\sigma}{d\Omega} = \frac{\alpha^2 E'}{4E^3 \sin^4(\Theta_e/2)} \left[A(Q^2)\cos^2(\Theta_e/2) + B(Q^2)\sin^2(\Theta_e/2)\right] \qquad (1.1)$$

where E and E' are the incident and scattered electron energies, Θ_e is the electron scattering angle, $Q^2 = 4EE'\sin^2(\Theta_e/2)$ is the four momentum transfer squared and α is the fine structure constant. The elastic electric and magnetic structure functions $A(Q^2)$ and $B(Q^2)$ are given in terms of the charge, quadrupole and magnetic form-factors $F_C(Q^2)$, $F_Q(Q^2)$, $F_M(Q^2)$:

$$A(Q^2) = F_C^2(Q^2) + \frac{8}{9}\tau^2 F_Q^2(Q^2) + \frac{2}{3}\tau F_M^2(Q^2) \qquad (1.2)$$

$$B(Q^2) = \frac{4}{3}\tau(1+\tau)F_M^2(Q^2) \qquad (1.3)$$

where $\tau = Q^2/4M_d^2$, with M_d being the deuteron mass.

Figure 1 shows the existing data[1-6] on $A(Q^2)$ and $B(Q^2)$. The $A(Q^2)$ data exhibit a fast fall-off with increasing momentum transfers. The $B(Q^2)$ data are indicative of a predicted diffractive feature but they do not exclude a flattening at large momentum transfers. As has been pointed out in Ref. 6, the data for $Q^2 > 1.75$ (GeV/c)^2 are also consistent with a constant value of 1.2×10^{-8} ($\chi^2 = 1.0$ per degree of freedom), implying the need for improved measurements. Though

the high Q^2 SLAC data on $B(Q^2)$ join smoothly onto the lower Q^2 from Saclay and Bonn, there is an apparent disagreement between the high Q^2 SLAC data on $A(Q^2)$ and the low Q^2 CEA and Saclay data in the region where they overlap, as can be seen in Fig. 2, indicating the need for further investigations.

The separation of the charge and quadrupole form-factors requires an additional polarization experiment.[7] One can measure the tensor (vector) polarization of the recoil deuteron with an unpolarized (polarized) electron beam and a polarimeter or use a polarized deuteron target. Such novel measurements have untangled, using a tensor polarimeter[8,9] or a tensor-polarized target,[10,11] F_C and F_Q up to Q^2=0.8 (GeV/c)^2, and have uncovered[9] the long predicted diffraction minimum of the charge form-factor.

In the nonrelativistic impulse approximation (NRIA) the deuteron form-factors are described in terms of the deuteron wave function and the electromagnetic form-factors of the nucleons.[12] Theoretical calculations based on the NRIA approach using various nucleon-nucleon potentials and parametrizations of the nucleon form-factors generally underestimate the $A(Q^2)$ data. They predict the diffraction minimum of $B(Q^2)$ but fail to describe simultaneously a) the data in the range $1.0 < Q^2 < 1.8$ (GeV/c)^2 and b) the location of the minimum and the height of the secondary maximum as can be seen[13] in Fig. 3.

Relativistic impulse approximation calculations (RIA) solving the Bethe-Salpeter equation slightly improve or worsen the agreement with the data depending on the approach taken.[14,15] Considerable improvement is provided by some recent relativistic impulse approximation calculations using light-front dynamics[16,17] for some particular choices of nucleon-nucleon potentials and nucleon form-factor parametrizations. A typical example is given in Fig. 4.

It has long been recognized that the form-factors of the deuteron are very sensitive to the presence of meson-exchange currents (MEC) and isobar configurations (IC). There have been numerous extensive studies and calculations augmenting both the nonrelativistic and relativistic approaches with the inclusion of MEC and

IC. The principal uncertainty in these calculations are the sign and the poorly known value of the $\gamma\pi\rho$ coupling constant[18] and the admixture of isobar states in the deuteron wave function. The inclusion of MEC and IC brings the theory in better agreement with the data, within the large theoretical and experimental uncertainties. There are many examples[19-21] of calculations describing successfully either both $A(Q^2)$ and $B(Q^2)$ or one of the two as can be seen in Figs. 5, 6, and 7 for NRIA and RIA approaches. It should be noted that the theoretical work of Fig. 6 finds the NRIA $B(Q^2)$ diffraction minimum filled up by MEC, a notion that is also consistent with the data.

It is widely recognized that at distances much less than the nucleon size, the underlying quark-gluon dynamics can not be ignored. This has lead in the formulation of the so called hybrid quark models that try to simultaneously incorporate the quark- and gluon-exchange mechanism at short distances and the meson-exchange mechanism at long and intermediate distances. A commonly used approach divides the deuteron in two regions: an exterior one described by baryon configurations and an interior one described by a quark cluster. When the internucleon separation becomes smaller than $\sim$ 1 fm the deuteron is treated as a six-quark configuration with a certain probability. Hybrid models[22,23] are able in general to describe well the $A(Q^2)$ and/or $B(Q^2)$ data as can be seen in Figs. 8 and 9. They are still in a phenomenological stage but the hope is that they could provide a consistent basis of bridging the meson-nucleon and quark-gluon descriptions.

At sufficiently large momentum transfers the form-factors should be calculable in terms of only quarks and gluons within the framework of QCD. There are presently perturbative QCD calculations predicting[24,25] the Q^2 dependence of the deuteron form-factors. The magnetic and charge form-factor data are inconsistent with such calculations that predict a smooth form-factor fall-off with increasing Q^2. These data seem to indicate that perturbative QCD calculations are not applicable for momentum transfers less than 2.5 $(\mathrm{GeV/c})^2$. In contrast, the $A(Q^2)$ SLAC data exhibit some evidence for asymptotic fall-off behavior for $Q^2 > 3$ $(\mathrm{GeV/c})^2$ as shown in Fig. 10.

This proposal aims to a better understanding of the deuteron structure by exploring the limits of elastic electron scattering that can be achieved with the unique features of the CEBAF machine and spectrometers. The objectives of this initiative are:

- To remeasure the electric elastic structure function $A(Q^2)$ in the Q^2 range covered at SLAC to resolve the apparent difference between the existing CEA/Saclay/Bonn and SLAC data and extend the measurements up to about Q^2=6 (GeV/c)^2.
- To improve significantly the existing SLAC data on the magnetic elastic structure function $B(Q^2)$ around its diffraction minimum and extend them to the highest possible Q^2, with a cross section sensitivity of 2×10^{-42} cm^2/sr.

The expected precision of the proposed data as well the new measurements on the nucleon electromagnetic form-factors from SLAC experiment NE11[26] should provide severe constraints in the theoretical calculations of the electromagnetic structure of the two body nuclear system. These new data will offer unique grounds for testing models of the nucleon-nucleon interaction, meson-exchange currents, isobar configurations and the possible influence of quark degrees of freedom. The need for these new measurements for the advancement of modern nuclear physics is universally accepted as expressed **'we need to extend all these type of measurements to higher momentum transfer'** in the recent DOE/NSF Long Range Plan.[27]

2. EXPERIMENT REQUIREMENTS

2.1 FORWARD ANGLE MEASUREMENT

The fast fall-off of both the Mott cross section and $A(Q^2)$ with increasing Q^2 requires the use of the largest possible target for maximizing the counting rate. The resulting degradation in missing mass resolution makes it impossible to separate elastic from inelastic scattering without detecting the recoiling deuterons in coincidence with the scattered electrons.

The two electron and hadron High Resolution Spectrometers (HRS) of Hall-A, shown schematically in Fig. 11 are the ideal devices to carry out such a coincidence measurement. The scattered electrons will be identified by the detector package of the electron HRS. The electron-deuteron coincidences will be identified by time-of-flight measurement between the electron trigger signal and a deuteron signal. The deuteron detection will require a subset of the hadron HRS detector package, consisting of two planes of scintillators and the drift chambers.

The excellent HRS resolutions and the small energy spread of the CEBAF beam allow single arm elastic scattering measurements at low Q^2 with a special short target cell. These measurements will provide detailed consistency and calibration checks of the double-arm perspective.

2.2 180° MEASUREMENT

The previous measurements at SLAC have shown that for Q^2 >1.5 $(\mathrm{GeV/c})^2$ the electric structure function is 2 to 3 orders of magnitude greater than the magnetic one, dictating that **any future $B(Q^2)$ measurements with Q^2 >1.5 $(\mathrm{GeV/c})^2$ have to be performed around 180°** so that the contributions from $A(Q^2)$ would not dominate.

The cross sections to be measured are known to be small and of the order of 10^{-41} to 10^{-42} $\mathrm{cm}^2/\mathrm{sr}$, necessitating a medium resolution electron spectrometer with the largest possible solid angle and the longest possible target consistent

with cryogenic limitations. The use of long targets introduces large energy losses to the incident and back-scattered electrons and degrades the missing mass resolution dictating that the recoil deuterons should be detected in coincidence in a spectrometer centered around 0°.

The required 180° electron spectrometer system would have to be built from existing surplus magnets at CEBAF or at other national laboratories such as SLAC. The hadron HRS of Hall A or the High Momentum Spectrometer (HMS) of Hall-C are ideal choices for the required 0° system in conjunction with a chicane of dipole magnets for transporting the incident electrons to the beam dump.

The identification of the electron-deuteron coincidences will rely on the double-arm time-of-flight measurement. The electron detection package will be assembled by detectors existing at CEBAF or loaned from other laboratories. The deuteron detection will require a subset of the full HRS or HMS detector packages. Two planes of scintillators and the drift chambers would suffice for the time-of-flight measurement and the reconstruction of the deuteron momentum and recoil angle.

The double-arm electron-deuteron coincidences from two-step photoproduction background processes observed in the SLAC experiment[6] will be significantly suppressed in this experiment. The resolutions of both electron and hadron spectrometers are adequate to apply strict cuts in the angular correlation of the scattered and recoil particles, *not applied in the SLAC experiment.* The background can be also reduced by using shorter target lengths compared to those used at SLAC.

2.3 TARGET

The experiments will require the high power liquid deuterium and hydrogen target system being designed and constructed by the C.S.U. (LA) group and J. Mark (SLAC) for Hall-A with a dual target cell. The optimum target length for both forward and backward angle measurements is 14 cm. The power dissipation for 100 μA incident beam current will be about 480 W, within the cooling capabilities of the planned refrigeration system of the CEBAF cryotarget. This length

will also suppress the double-arm background coincidences induced in the target by bremsstrahlung photons by at least a factor of two as compared to the SLAC experiment. A shorter target cell would be also necessary for consistency and calibration checks.

3. THE 180°/0° SPECTROMETER SYSTEM

3.1 OVERVIEW

Our proposed 180° electron spectrometer system is similar to that used in the SLAC experiment NE4[28] and is shown schematically in Fig. 12. The back-scattered electrons are focused in the quadrupole doublet Q4−Q5 and momentum analyzed and transported to a set of detectors by the dipole magnets D4−D5. The incident electron beam travels through the 'chicane' of dipole magnets D2−D3−D4 and then through the magnetic axis of the quadrupole doublet before impinging on the target. The target is moved ~1.5 m upstream from its nominal position on the Hall-A or Hall-C pivot.

The recoil deuterons or protons are deflected towards the Hall-A hadron HRS or the Hall-C HMS spectrometer by the 'split' dipole magnet D6, as shown in Fig. 13. The transmitted beam, which is degraded by radiation, ionization and multiple scattering, is directed towards the beam dump of the Hall through the chicane of dipole magnets D6−D7−D8.

The electrical power required for the extra magnets of this experiment will require both high voltage transformers of Hall-A and Hall-C. The power supplies needed could be provided from other experimental facilities such as the SOS spectrometer, the Hall-A beam polarization chicane etc. More units if needed, can be acquired from other laboratories with available surplus power supplies.

3.2 THE 180° ELECTRON SPECTROMETER

To maximize the solid angle of the electron spectrometer, quadrupoles with the shorter length and wider aperture possible should be used. These requirements are met by the surplus 10Q18 quadrupoles from the Argonne ZGS currently available from SLAC. The same magnets were used in the SLAC experiment NE4.

The two dipole magnets should be of a fairly good field uniformity to fulfill the modest resolution requirements and with gaps comparable to the apertures of the quadrupoles to preserve their gathering power. The 29D36 surplus magnets from the Berkeley bevatron are ideal candidates and can be run in series by a single power supply. Two of these dipoles were also used in the SLAC experiment.

The optics of the electron spectrometer is parallel-to-point in the non-bend plane and point-to-point in the bend plane. The resulting resolutions are adequate for the needs of the experiment. The momentum resolution will be $< 0.4\%$ and the angular resolutions $\sim \pm 5$ mr in the non-bend plane and $\sim \pm 7$ mr in the bend plane.

In an effort to reduce the required extra magnets and power supplies, we are currently investigating the possibility of using just a quadrupole doublet spectrometer for detecting the 180° back-scattered electrons. This option will require two quadrupoles strong enough (such as the SLAC 15Q51) to provide point-to-point focusing in both planes. Proper collimation would allow transmission to a set of detectors only of elastic electron events originating from the target.

Another possible option under investigation is the use of a magnetic flux exclusion shield around the incident beam axis inside magnet D4. In this case the incident beam will travel through magnet D4 undeflected towards the target eliminating the need for magnets D2 and D3. This arrangement will reduce the complexity of the spectrometer system and increase the running efficiency. Preliminary calculations have shown[29] that several concentric layers of proper materials could reduce a 7 kG field to a ~5 G level inside the shield. This field strength introduces negligible deflection to the incident electron beam.

3.3 THE 0° RECOIL SPECTROMETER

The recoiling deuterons will be detected either in the Hall-C HMS or in the Hall-A hadron HRS. The HMS choice will require a simple change in the Q1−Q2−Q3 quadrupole settings. The hadron HRS choice will also require an alternate optics tune, where the Q1−Q2 quadrupoles are pushed downstream by ∼1 m towards the dipole magnet D1. The deuteron spectrometer will point for all kinematical settings towards the center of the split magnet D6 which will deflect the recoiling nuclei by a fixed angle $< 12°$.

The gap of magnet D6 in the vertical direction should be about 20 cm, not limiting the angular acceptance of the deuteron spectrometer which is for both the HRS or HMS options ∼50 mr. The width of the magnet should be wide enough to accommodate both mutually diverging beams of recoiling nuclei and electrons. For a standard magnet length of 91 cm (36 in) the required width is 50 cm. A 29D36 Berkeley surplus magnet is a satisfactory choice for D6 and D8 running in series by a single power supply.

The bend plane optics of HRS or HMS will be preserved, with the exception of some calculable focusing from the exit pole face rotation of magnet D6. In the horizontal plane this magnet will introduce some coupling between relative momentum and production angle. The resulting degradation in the momentum and angular resolutions is much smaller than that caused by multiple scattering and energy loss effects and will not be a limiting factor in the reconstruction of the production coordinates of the recoiling nuclei.

3.4 THE BEAM CHICANES

The incident electron beam, after exiting the beam switchyard, is transmitted to the target through the upstream chicane of D2−D3−D4 dipoles. Standard surplus bending magnets such as 18D36 can be utilized in place of D2 and D3. Magnet D2 deflects the beam by the same angle as D4. Magnet D3 is placed symmetrically along the beam direction with respect to D2 and D4, and its deflection angle is

twice the deflection angle of magnets D2 and D4. The symmetric arrangement and operation of this chicane preserves the initial achromaticity of the electron beam. The horizontal position of D3 is adjusted as necessary to accommodate different kinematic settings.

The incident electron beam after passing through the target will be directed to the beam dump of Hall-A or Hall-C through the downstream chicane of dipole magnets D6–D7–D8. The horizontal position of magnet D7 is also adjusted to accommodate different beam energies. This chicane is also an achromatic magnet system so that the position and divergence of the electrons at the exit of the chicane do not depend on their momentum. The phase space of the beam going to the dump will be the same as in an ordinary electron scattering experiment with the beam going straight from the target to the dump.

A small fraction of the beam (~2%) degraded by bremsstrahlung and ionization energy losses in the target will be deflected onto the vacuum pipe walls of the downstream chicane. The deposited power is of the order of 2 to 3 kW and will require part of the chicane vacuum pipe to be water cooled. To minimize the background created by the part of the beam hitting the vacuum walls, the downstream beam chicane will have to be shielded by concrete blocks.

4. RUN PLAN-COUNTING RATES

4.1 THE FORWARD ANGLE EXPERIMENT

The proposed kinematics for the forward scattering angle $A(Q^2)$ experiment is given in Table 1. The cross sections are based on a fit to the SLAC $A(Q^2)$ data from experiment E101.[5] The small contribution of $B(Q^2)$ has been estimated assuming that it follows the 'optimistic' $B(Q^2)$ scenario described in next section. The calculated rates are given in Table, 2 assuming 100 μA beam current, a 14 cm long liquid deuterium target. a solid angle of 7 msr for HRS and a radiative correction factor of 0.7. The rates have taken into account the mismatch of the

electron and deuteron solid angles for $Q^2 < 4$ (GeV/c)^2 given by the sixth column of Table 1.

The estimated required time to measure $A(Q^2)$ to the maximum Q^2 possible with a sensitivity limit of $\sim \pm 25\%$ statistical uncertainty in 3 days of beam time is 22 days. The quality of the projected possible data under the above assumptions is shown in Fig. 14. The projected total systematic error will be about $\sim \pm 5\%$, dominated by the uncertainties in a) the calculation of the double-arm solid angle ($\sim \pm 3\%$) and b) the correction for deuteron losses in the target and in the detectors ($\sim \pm 3\%$).

The performance of the double-arm HRS system will be checked out with elastic electron-proton scattering. It is estimated that about 3 calendar days will be required for calibration runs and for periodic checks of the detectors using double-arm elastic electron-proton scattering. Assuming a 50% overall experimental efficiency, the required running time to measure $A(Q^2)$ is 25 days. An additional 5 days of initial check-out time will be also necessary to debug the online software, electronics etc., resulting in a total time request of one calendar month.

4.2 180° SCATTERING EXPERIMENT

The kinematical parameters of 180° elastic electron-deuteron scattering are given in Table 3 for the Q^2 range 0.5 to 5.0 (GeV/c)^2. The backward scattering cross sections are roughly known up to Q^2=2.5 (GeV/c)^2. For higher momentum transfers we have assumed two arbitrarily named scenarios: (1) an 'optimistic' one predicting a relatively slow magnetic form-factor fall-off as in the Dijk and Bakker model[23] and (2) a 'pessimistic' one predicting that the magnetic form-factor drops very fast with Q^2 as in one of the Blunden *et. al.*[22] models.

In estimating the counting rates and required run times we have assumed a beam current of 100 μA, a deuterium target length of 14 cm, a double-arm solid angle of 18 msr and a radiative correction factor of 0.7. For both cases we assume that the maximum $B(Q^2)$ statistical error will be $\sim \pm 35\%$ in a week of beam time.

The projected total systematic error will be, as in the $A(Q^2)$ measurement, about $\pm 5\%$ dominated by similar uncertainties.

The estimated required time to measure $B(Q^2)$ to the maximum Q^2 possible and map accurately its diffraction minimum is 26.5 days at 100% efficiency as can be seen in Tables 4 and 5. The quality of the projected data possible under the above assumptions is shown for the optimistic scenario in Fig. 15 and for the pessimistic one in Fig. 16.

A fair amount of beam time is also required for measuring elastic electron-proton scattering. It is estimated that 7 calendar days of hydrogen running will be necessary to understand and check periodically the performance of the double-arm spectrometer system. Assuming 40% overall experimental efficiency, the total amount of running time to perform this *one time operation* perspective is two and half calendar months. Our experience from the SLAC experiment suggests that two weeks of check-out will be required for debugging the double-arm spectrometer system and detectors.

5. SUMMARY–REQUEST

We propose to improve the existing data on the elastic electric $A(Q^2)$ and magnetic $B(Q^2)$ structure functions of the deuteron and extend them to the highest Q^2 possible. The results are expected to provide a better understanding of the structure of the deuteron in terms of nucleonic, mesonic and possibly quark degrees of freedom.

The facilities needed to carry out the measurement of $A(Q^2)$ will be available in the early phase of the Hall-A operations. Specifically we request use of a) the electron and hadron High Resolution Spectrometers, b) the high power liquid deuterium/hydrogen target system of Hall-A, c) the data acquisition system of Hall-A and d) 25 days of beam time calculated with 50% efficiency and 5 days of checkout.

The $B(Q^2)$ measurement will require additional equipment, not planned in the CEBAF CDR. Most of this equipment is available from other laboratories and could be transported to CEBAF at a minimal cost. This measurement can be performed in either Hall-A or Hall-C. The choice should involve prior detailed consultations with the CEBAF Management and Staff and should have the minimum impact to the rest of the experimental program. The setup of the extra apparatus could take place during periods requiring exclusive use of the accelerator by one of the other Halls (e.g. polarization experiments). The beam time required for the 180° experiment is two and half months of data taking at 40% efficiency and two weeks of checkout.

TABLE CAPTIONS

1: Elastic electron-deuteron kinematics in the squared four momentum transfer range 1.0 to 6.0 $(\mathrm{GeV/c})^2$. The incident electron energy is fixed at 4 GeV. E' and Θ_e are the scattered electron energy and angle. P_d and Θ_d are the recoil deuteron momentum and angle. The last column is the ratio of the electron to deuteron solid angle elements.

2: Possible run plan scenario with cross section estimates and counting rates for the $A(Q^2)$ measurement. The run plan is based on a fit to the SLAC $A(Q^2)$ data from experiment E101.[5] The rate estimates assume a 14 cm long liquid deuterium target, a beam current of 100 μA, 7 msr solid angle for HRS and a radiative correction factor of 0.7.

3: Elastic electron-deuteron kinematics in the four momentum transfer range 0.5 to 5.0 $(\mathrm{GeV/c})^2$. The electron scattering angle Θ_e is fixed at 180°. E is the incident beam energy, E' is the scattered electron energy, P_d is the recoil deuteron momentum. The last column is the ratio of the electron to deuteron solid angle elements.

4: An optimistic run plan scenario with cross section estimates and counting rates for the $B(Q^2)$ measurement. The run plan assumes a slow $B(Q^2)$ fall-off for Q^2 >2.5 $(\mathrm{GeV/c})^2$ as in the Dijk and Bakker model.[23] The rate estimates assume a 14 cm long liquid deuterium target, a beam current of 100 μA, a double-arm solid angle of 18 msr and a radiative correction factor of 0.7.

5: A pessimistic run plan scenario with cross section estimates and counting rates for the $B(Q^2)$ measurement. The run plan assumes a fast $B(Q^2)$ fall-off for Q^2 >2.5 $(\mathrm{GeV/c})^2$ as in one of the Blunden *et. al.* models.[22] The rate estimates assume a 14 cm long liquid deuterium target, a beam current of 100 μA, a double-arm solid angle of 18 msr and a radiative correction factor of 0.7.

TABLE 1

ELECTRON-DEUTERON ELASTIC KINEMATICS

$E = 4$ GeV

Q^2 $(\mathrm{GeV/c})^2$	E' GeV	Θ_e deg.	P_d GeV/c	Θ_d deg.	$\Delta\Omega_e/\Delta\Omega_d$
1.00	3.733	14.87	1.035	67.77	0.203
1.25	3.667	16.79	1.167	65.19	0.241
1.50	3.600	18.57	1.288	62.88	0.281
1.75	3.533	20.27	1.403	60.76	0.323
2.00	3.467	21.89	1.511	58.79	0.367
2.25	3.400	23.47	1.615	56.95	0.414
2.50	3.334	25.01	1.716	55.21	0.464
2.75	3.267	26.52	1.813	53.57	0.519
3.00	3.200	28.02	1.908	51.99	0.577
3.50	3.067	30.98	2.091	49.04	0.709
4.00	2.934	33.95	2.267	46.28	0.864
4.50	2.800	36.95	2.437	43.69	1.047
5.00	2.667	40.03	2.603	41.23	1.267
5.50	2.534	43.22	2.766	38.86	1.530
6.00	2.401	46.56	2.925	36.57	1.849

TABLE 2

$A(Q^2)$ RUN PLAN SCENARIO

$E = 4$ GeV

Target = 14 cm Liquid Deuterium

Current = 100 μA

$\Delta\Omega = 7$ msr

Q^2 $(GeV/c)^2$	$A(Q^2)$	Cross Section (cm^2/sr)	Time (hour)	Counts	$\Delta A(Q^2)$ (±%)
1.00	9.97×10^{-5}	1.06×10^{-34}	1	10000	1
1.25	4.58×10^{-5}	2.93×10^{-35}	1	10000	1
1.50	2.16×10^{-5}	9.05×10^{-36}	1	10000	1
1.75	1.05×10^{-5}	3.03×10^{-36}	2	10000	1
2.00	5.23×10^{-6}	1.09×10^{-36}	3	10000	1
2.25	2.68×10^{-6}	4.14×10^{-37}	5	10000	1
2.50	1.41×10^{-6}	1.66×10^{-37}	5	2500	2
2.75	7.67×10^{-7}	6.96×10^{-38}	5	1100	3
3.00	4.28×10^{-7}	3.05×10^{-38}	8	1100	3
3.50	1.45×10^{-7}	6.67×10^{-39}	11	400	5
4.00	5.47×10^{-8}	1.71×10^{-39}	19	230	7
4.50	2.31×10^{-8}	5.09×10^{-40}	25	100	11
5.00	1.09×10^{-8}	1.68×10^{-40}	34	44	17
5.50	5.75×10^{-9}	6.07×10^{-41}	52	25	22
6.00	3.39×10^{-9}	2.40×10^{-41}	86	16	27
TOTAL			258		
TOTAL	50%	Efficiency	516		

TABLE 3

ELECTRON-DEUTERON ELASTIC KINEMATICS

$\Theta_e = 180°$

Q^2 $(GeV/c)^2$	E GeV	E' GeV	P_d GeV/c	$\Delta\Omega_e/\Delta\Omega_d$
0.5	0.426	0.293	0.720	6.02
1.0	0.651	0.384	1.035	7.25
1.5	0.844	0.444	1.288	8.40
2.0	1.022	0.489	1.511	9.52
2.5	1.191	0.525	1.716	10.6
3.0	1.354	0.554	1.908	11.9
3.5	1.512	0.579	2.090	13.0
4.0	1.666	0.600	2.266	14.3
4.5	1.818	0.619	2.437	15.6
5.0	1.968	0.635	2.603	16.7

TABLE 4

OPTIMISTIC $B(Q^2)$ RUN PLAN SCENARIO

$\theta = 180°$

Target = 14 cm Liquid Deuterium

Current = 100 μA

$\Delta\Omega$ = 18 msr

Q^2 $(GeV/c)^2$	$B(Q^2)$	Cross Section (cm^2/sr)	Time (hour)	Counts	$\Delta B(Q^2)$ (±%)
1.1	3.94×10^{-6}	2.52×10^{-38}	1	400	5
1.2	2.28×10^{-6}	1.28×10^{-38}	2	400	5
1.3	1.25×10^{-6}	6.27×10^{-39}	3	400	5
1.4	6.39×10^{-7}	2.89×10^{-39}	7	400	5
1.5	2.94×10^{-7}	1.23×10^{-39}	16	400	6
1.6	1.19×10^{-7}	4.77×10^{-40}	22	200	9
1.7	4.10×10^{-8}	1.74×10^{-40}	29	100	14
1.8	1.18×10^{-8}	6.49×10^{-41}	77	100	20
2.0	8.08×10^{-9}	3.43×10^{-41}	65	44	27
2.3	1.32×10^{-8}	3.00×10^{-41}	42	25	24
2.6	1.84×10^{-8}	2.97×10^{-41}	42	25	22
3.0	2.26×10^{-8}	2.68×10^{-41}	40	21	22
3.5	1.99×10^{-8}	1.74×10^{-41}	46	16	25
4.0	1.13×10^{-8}	7.68×10^{-42}	72	11	30
4.5	4.21×10^{-9}	2.27×10^{-42}	168	6	37
TOTAL			632		
TOTAL	40%	Efficiency	1580		

TABLE 5

PESSIMISTIC $B(Q^2)$ RUN PLAN SCENARIO

$\theta = 180°$

Target = 14 cm Liquid Deuterium

Current = 100 μA

$\Delta\Omega$ = 18 msr

Q^2 (GeV/c)^2	$B(Q^2)$	Cross Section (cm^2/sr)	Time (hour)	Counts	$\Delta B(Q^2)$ ($\pm$%)
1.1	3.94×10^{-6}	2.52×10^{-38}	1	400	5
1.2	2.28×10^{-6}	1.28×10^{-38}	2	400	5
1.3	1.25×10^{-6}	6.27×10^{-39}	3	400	5
1.4	6.39×10^{-7}	2.89×10^{-39}	7	400	5
1.5	2.94×10^{-7}	1.23×10^{-39}	16	400	6
1.6	1.19×10^{-7}	4.77×10^{-40}	22	200	9
1.7	4.10×10^{-8}	1.74×10^{-40}	29	100	14
1.8	1.18×10^{-8}	6.49×10^{-41}	77	100	20
2.0	8.08×10^{-9}	3.43×10^{-41}	65	44	27
2.2	1.28×10^{-8}	3.33×10^{-41}	38	25	26
2.4	1.60×10^{-8}	3.16×10^{-41}	40	25	23
2.6	1.24×10^{-8}	2.07×10^{-41}	39	16	28
2.7	9.12×10^{-9}	1.43×10^{-41}	56	16	28
2.8	5.93×10^{-9}	8.88×10^{-42}	90	16	28
2.9	3.41×10^{-9}	5.02×10^{-42}	159	16	30
TOTAL			644		
TOTAL	40%	Efficiency	1610		

FIGURE CAPTIONS

1) The existing data on the elastic electric $A(Q^2)$ and magnetic $B(Q^2)$ structure functions for Q^2 >0.5 $(\mathrm{GeV/c})^2$. The measurements are from CEA, Saclay, Bonn and SLAC (Refs. 1−6). The dashed lines represent fits to the data.

2) Comparison of the available $A(Q^2)$ from SLAC[5], CEA[1] and Saclay[2] in the Q^2 range 0.5 to 2.0 $(\mathrm{GeV/c})^2$. The dashed curve is a fit to the combined CEA, Saclay and Bonn data. The solid line is a fit to all SLAC data in the range $0.8 < Q^2 < 4$ $(\mathrm{GeV/c})^2$.

3) a) The deuteron $A(Q^2)$ and $B(Q^2)$ structure functions calculated[13] in the impulse approximation, using several versions of the Bonn nucleon-nucleon potential;[30] b) with inclusion of relativistic corrections and meson-exchange currents.

4) The deuteron $A(Q^2)$ and $B(Q^2)$ structure functions of the relativistic model of Chung *et. al.*[16] using light-front dynamics for several potential models. Curves a) use the Höhler *et. al.* nucleon form-factors.[31] Curves b) use the Gari-Krümpelmann form-factors.[32]

5) Top: The deuteron $A(Q^2)$ and $B(Q^2)$ structure functions in the nonrelativistic impulse approximation formalism of Hummel and Tjon[19] with and without meson-exchange currents. The calculations used the nucleon form-factors of Ref. 31 and the Reid Soft Core[33] potential model. Bottom: Calculation within the Bethe-Salpeter and the relativistic quasipotential formalism of Hummel and Tjon with and without meson-exchange currents. The nucleon form-factors of Ref. 31 were used for all but the dotted-dashed line which is calculated with the form-factors of Ref. 32.

6) The deuteron $A(Q^2)$ and $B(Q^2)$ structure functions of Schiavilla and Risca,[21] using the Argonne V14 potential[34] and the nucleon form-factors of Ref. 31. The $B(Q^2)$ curves are calculated with different cutoff mass values in the πNN and ρNN vertex form-factors of the $\gamma\pi\rho$ MEC operator.

7) The deuteron $A(Q^2)$ and $B(Q^2)$ structure functions for two models with different isobar configurations by Dymarz and Khanna.[20] The dashed curve is the impulse approximation calculation. The dotted-dashed curve includes Δ currents. The solid curve is the full model that includes meson-exchange currents.

8) The deuteron $A(Q^2)$ and $B(Q^2)$ structure functions in the hybrid quark compound model of Dijk and Bakker[23] using the nucleon form-factors of Ref. 32. The dotted curve is the impulse approximation. The solid curve is the full model using the authors' fit to nucleon-nucleon scattering data. The dash-dotted curve is the full calculation with the Paris[35] potential.

9) The deuteron $A(Q^2)$ and $B(Q^2)$ structure functions in the hybrid model of Blunden *et. al.*[22] that includes MEC and $\Delta\Delta$ channels as well as quark admixtures. The curves are calculated for two different models with the nucleon form-factors of Ref. 31 (solid and dash-dotted curves) and of Ref. 32 (dashed and dotted curves).

10) Data for (a) $Q^{20}A(Q^2)$ from Ref. 5 and (b) $Q^{24}B(Q^2)$ from Ref. 6. In leading-order perturbative QCD these quantities should approach[24][25] a constant value at high Q^2.

11) The experimental setup for forward angle electron-deuteron scattering in coincidence showing the electron and hadron High Resolution Spectrometers (HRS) of Hall-A. The elements D1 are dipole and Q1$-$Q3 are quadrupole magnets. E, E' and P_d indicate the incident, scattered electron and recoil deuteron momenta. Θ_e and Θ_d stand for the scattered electron and recoil deuteron angles.

12) Schematic of the 180° electron spectrometer system and of the incident beam chicane. The elements Q4, Q5 are quadrupole and D2$-$D5 are dipole magnets. The open arrows indicate the path of the incident electrons. The solid arrows indicate the central trajectory of the back-scattered electrons.

13) Schematic of the recoil deuteron spectrometer system and the exit beam chicane using (a) the High Momentum Spectrometer (HMS) in Hall-C or (b) the hadron High Resolution Spectrometer (HRS) in Hall-A. The elements Q1−Q3 are quadrupole and the elements D1, D6−D8 are dipole magnets. The open arrows indicate the central trajectory of the recoiling deuterons and the solid arrows the path of the electron beam after passing through the target.

14) Projected possible data for the measurement of $A(Q^2)$ at CEBAF using the electron and hadron High Resolution Spectrometers of Hall-A in coincidence. The run plan assumes the ~7 msr solid angle of HRS, a 14 cm long deuterium cryotarget and 100 μA electron beam current. The required beam time is one calendar month including proton calibrations and checkout, assuming 50% data taking efficiency.

15) Projected possible data for the measurement of $B(Q^2)$ at CEBAF using a double-arm spectrometer system with a solid angle of 18 msr and with a 14 cm long deuterium cryotarget. The run plan assumes a slow $B(Q^2)$ fall-off for Q^2 >2.5 (GeV/c)^2 as in the Dijk and Bakker model[23] and will require about 75 days of data taking with 40% efficiency, including calibrations.

16) Projected possible data for the measurement of $B(Q^2)$ at CEBAF using a double-arm spectrometer system with a solid angle of 18 msr and with a 14 cm long deuterium cryotarget. The run plan assumes a fast $B(Q^2)$ fall-off for Q^2 >2.5 (GeV/c)^2 as in one of the Blunden *et. al.* models.[22] and will require about 75 days of data taking with 40% efficiency, including calibrations.

REFERENCES

[1] J. E. Elias *et. al.*, Phys. Rev. **177**, 2075 (1969).

[2] S. Platckov *et. al.*, Nucl. Phys. **A510**, 740 (1990).

[3] S. Auffret *et. al.*, Phys. Rev. Lett. **54**, 649 (1985).

[4] R. Cramer *et. al.*, Z. Phys. **C29**, 513 (1985).

[5] R. G. Arnold *et. al.*, Phys. Rev. Lett. **35**, 776 (1975).

[6] P. E. Bosted *et. al.*, Phys. Rev. **C42**, 38 (1990).

[7] J. Arvieux and J. M. Cameron, Advan. Nucl. Phys. **18**, 107 (1988).

[8] M. E. Schulze *et. al.*, Phys. Rev. Lett. **52**, 597 (1984).

[9] I. The *et. al.*, Phys. Rev. Lett. **67**, 173 (1991).

[10] V. M. Dmitriev *et. al.*, Phys. Lett. **B157**, 143 (1985); B. B. Voitsekhovskii *et. al.*, JETP Lett. **43**, 733 (1986).

[11] R. Gilman *et. al.*, Phys. Rev. Lett. **65**, 1733 (1990).

[12] E. L. Lomon, Ann. Phys. (N.Y.) **125**, 309 (1980).

[13] W. Plesas, in 4^{th} *Workshop On Perspectives In Nuclear Physics At Intermediate Energies*, Trieste, 1989, edited by S. Boffi, C. Ciofi degli Atti and M. Giannini (World Scientific, Teaneck, N.J., 1989).

[14] R. G. Arnold *et. al.*, Phys. Rev. **C21**, 1426 (1980).

[15] R. S. Bhalero and S. A. Gurvitz, Phys. Rev. **C24**, 2773 (1981).

[16] P. L. Chung *et. al.*, Phys. Rev. **C37**, 2000 (1988).

[17] L. L. Frankfurt *et. al.*, Phys. Rev. Lett. **62**, 387 (1989).

[18] P. Sarriguren *et. al.*, Phys. Lett. **B228**, 285 (1989).

[19] E. Hummel and J. A. Tjon, Phys. Rev. **C42**, 423 (1990).

[20] R. Dymarz and F. C. Khanna, Nucl. Phys. **A516**, 549 (1990).

[21] R. Schiavilla and D. O. Riska, Phys. Rev. **C43**, 437 (1991).

[22] W. P. Sitarski *et. al.*, Phys. Rev. **36**, 2479 (1987); P. G. Blunden *et. al.*, Phys. Rev. **C40**, 1541 (1989).

[23] H. Dijk and B. L.G. Bakker, Nucl. Phys. **A494**, 438 (1989).

[24] S. Brodsky *et. al.*, Phys. Rev. Lett. **51**, 83 (1983).

[25] C. E. Carlson and F. Gross, Phys. Rev. Lett. **53**, 127 (1984).

[26] P. E. Bosted, private communication.

[27] *Nuclear Science in the 1990's*, DOE/NSF Long Range Plan, p. 23 (1989).

[28] G. G. Petratos, SLAC Report NPAS-TN-86-7 (1986); A. T. Katramatou *et. al.*, Nucl. Instr. Meth. **A267**, 448 (1988).

[29] S. St. Lorant, private communication.

[30] R. Machleidt *et. al.*, Phys. Rep. **149**, 1 (1987)

[31] G. Höhler *et. al.*, Nucl. Phys. **B114**, 505 (1976).

[32] M. Gari and W. Krümpelmann, Phys. Lett. **B173**, 10 (1986).

[33] R. V. Reid, Ann. Phys. (N.Y.) **50**, 411 (1968).

[34] R. B. Wiringa *et. al.*, Phys. Rev. **C29**, 1207 (1984).

[35] M. Lacombe *et. al.*, Phys. Rev. **C21**, 861 (1980).

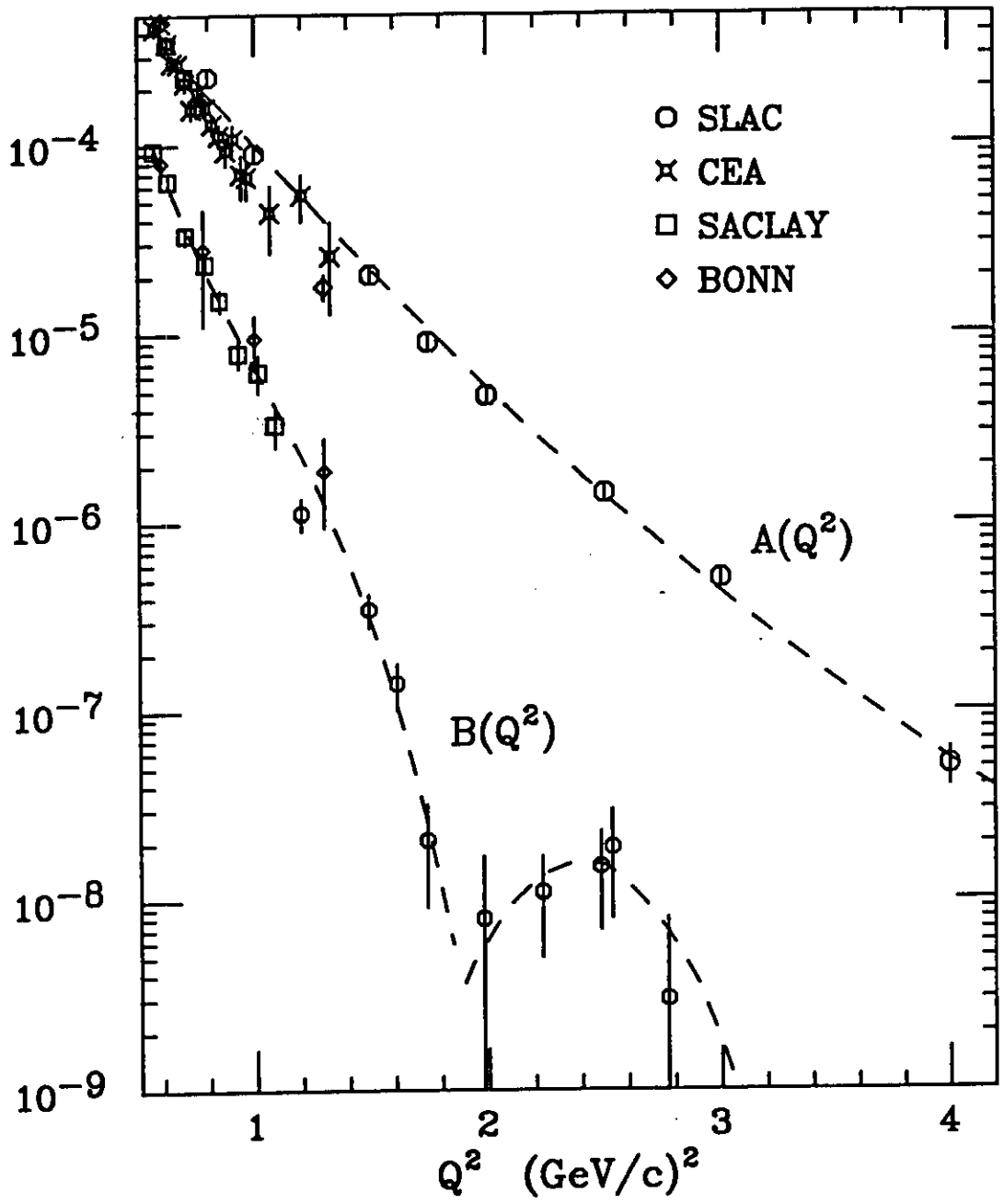
SLAC
CEA
SACLAY
BONN
$A(Q^2)$
$B(Q^2)$
10^{-4}
10^{-5}
10^{-6}
10^{-7}
10^{-8}
10^{-9}
1
2
3
4
Q^2 $(GeV/c)^2$

FIGURE 1

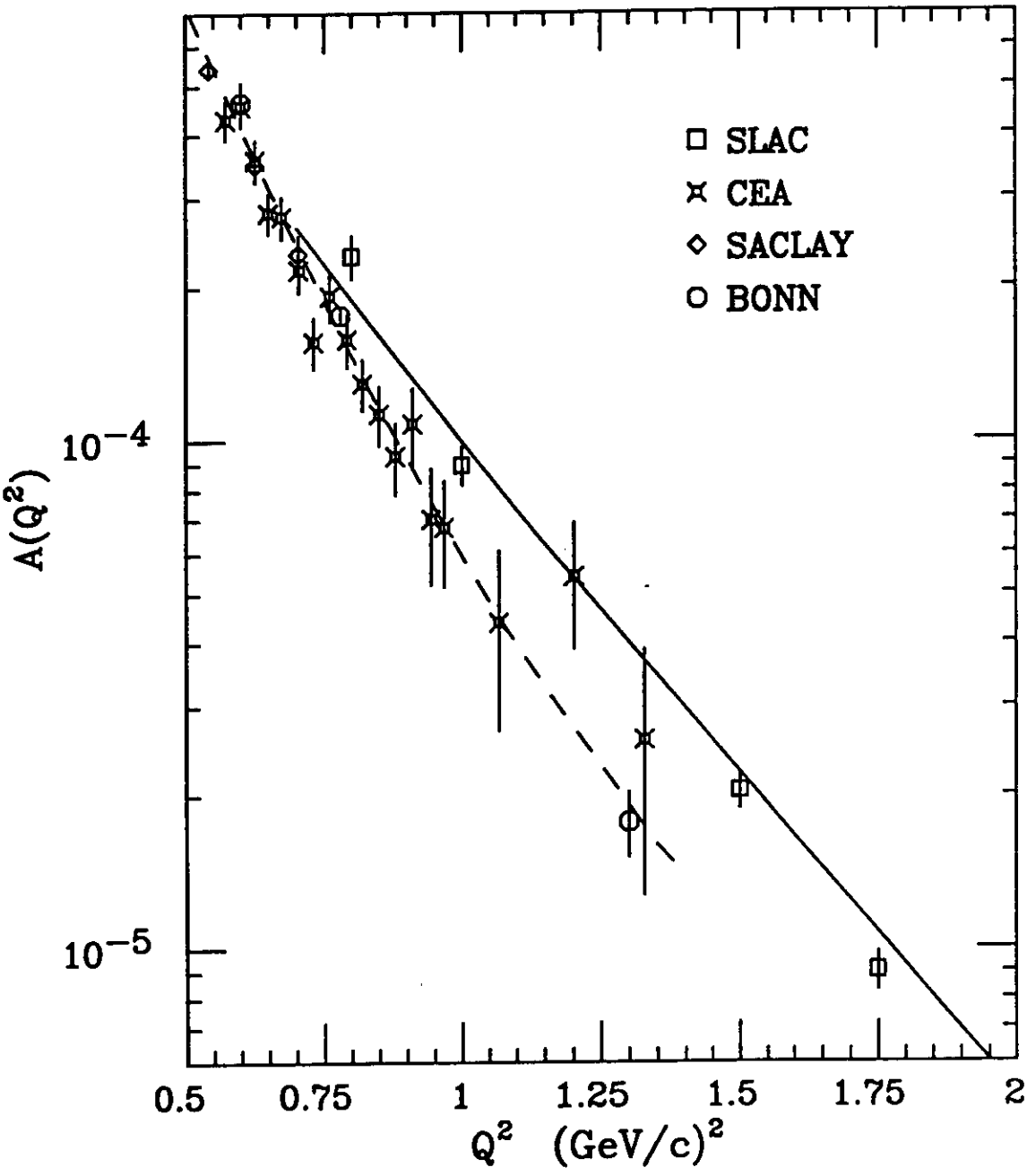

FIGURE 2

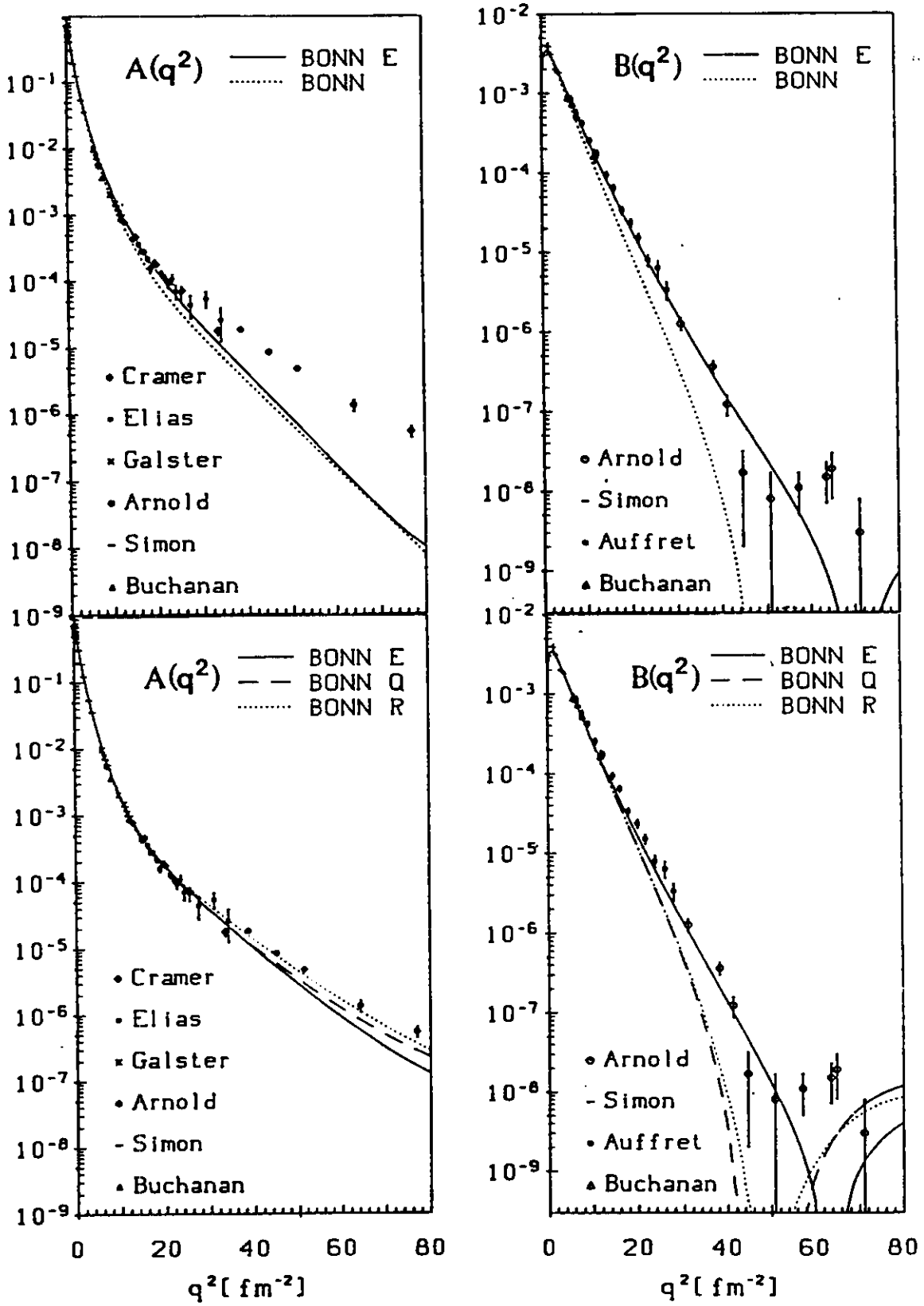
A(q²)
BONN E
BONN
• Cramer
• Elias
× Galster
• Arnold
- Simon
▲ Buchanan
B(q²)
BONN E
BONN
• Arnold
- Simon
• Auffret
▲ Buchanan
A(q²)
BONN E
BONN Q
BONN R
• Cramer
• Elias
× Galster
• Arnold
- Simon
▲ Buchanan
B(q²)
BONN E
BONN Q
BONN R
• Arnold
- Simon
• Auffret
▲ Buchanan
0 20 40 60 80
q²[fm⁻²]
0 20 40 60 80
q²[fm⁻²]

FIGURE 3

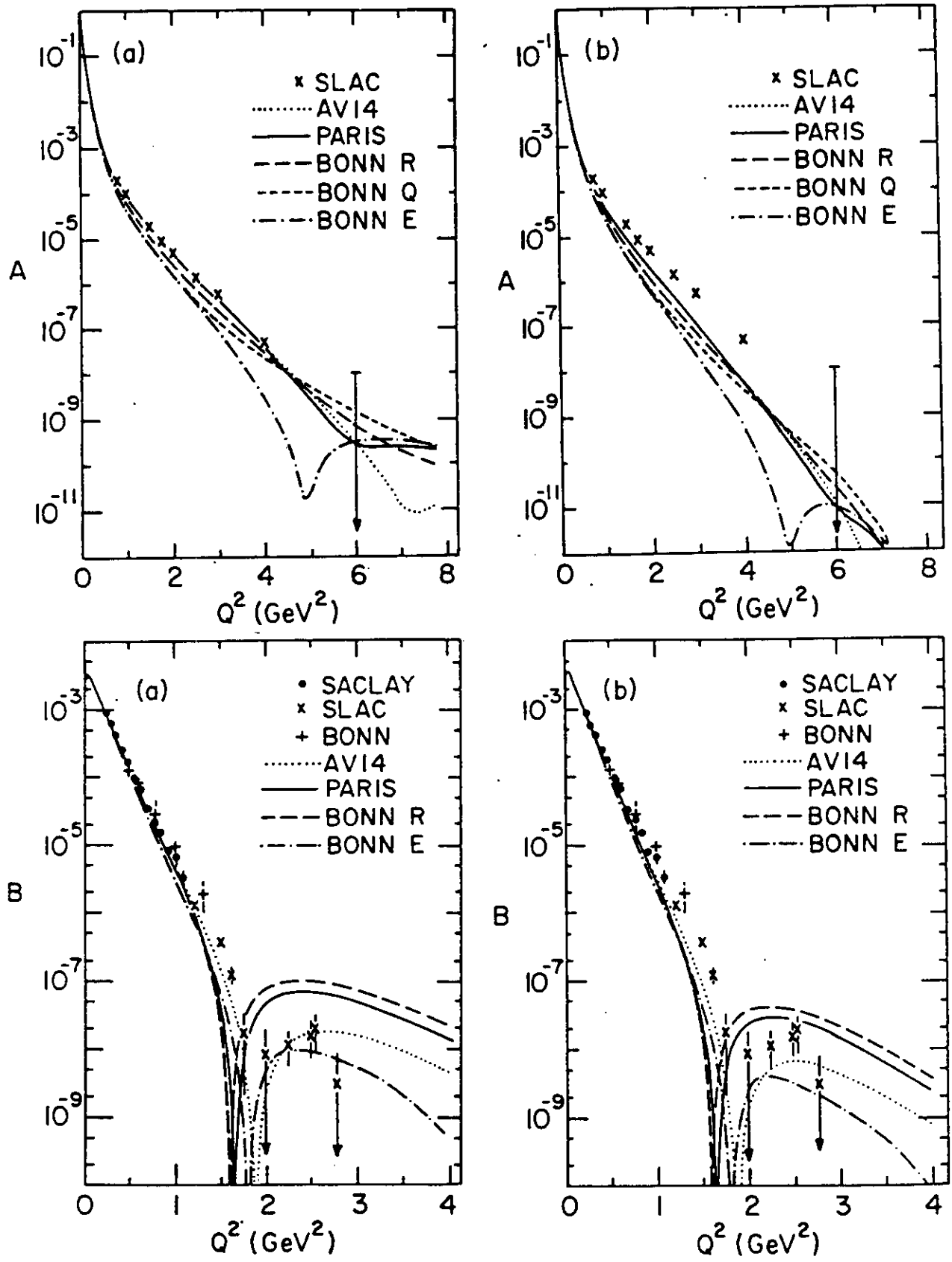
(a)
SLAC
AV14
PARIS
BONN R
BONN Q
BONN E
A
Q^2 (GeV^2)
(b)
SLAC
AV14
PARIS
BONN R
BONN Q
BONN E
A
Q^2 (GeV^2)
(a)
SACLAY
SLAC
BONN
AV14
PARIS
BONN R
BONN E
B
Q^2 (GeV^2)
(b)
SACLAY
SLAC
BONN
AV14
PARIS
BONN R
BONN E
B
Q^2 (GeV^2)

FIGURE 4

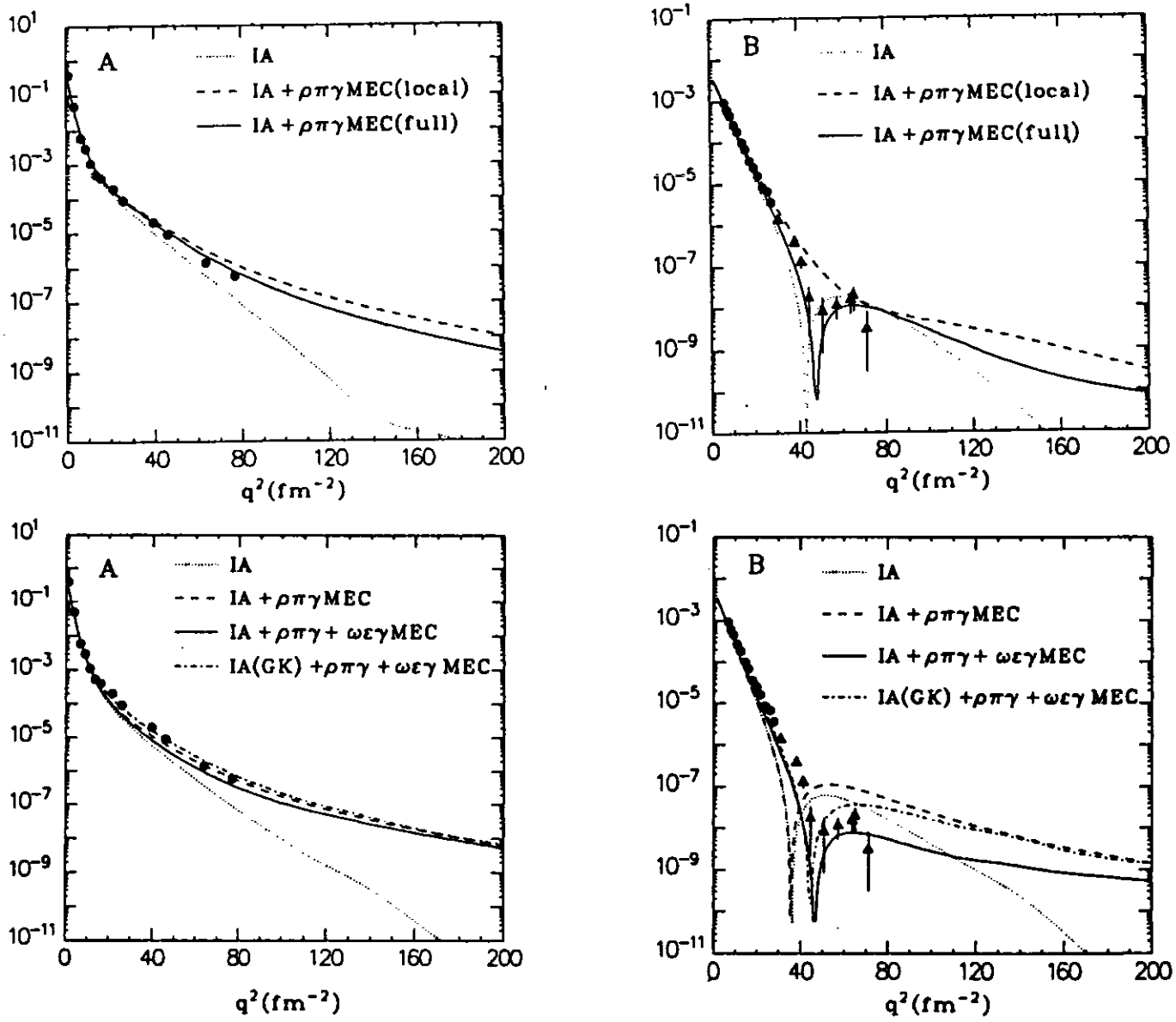
A
IA
IA + ρπγMEC(local)
IA + ρπγMEC(full)
B
IA
IA + ρπγMEC(local)
IA + ρπγMEC(full)
A
IA
IA + ρπγMEC
IA + ρπγ + ωεγMEC
IA(GK) + ρπγ + ωεγ MEC
B
IA
IA + ρπγMEC
IA + ρπγ + ωεγMEC
IA(GK) + ρπγ + ωεγ MEC
q²(fm⁻²)

FIGURE 5

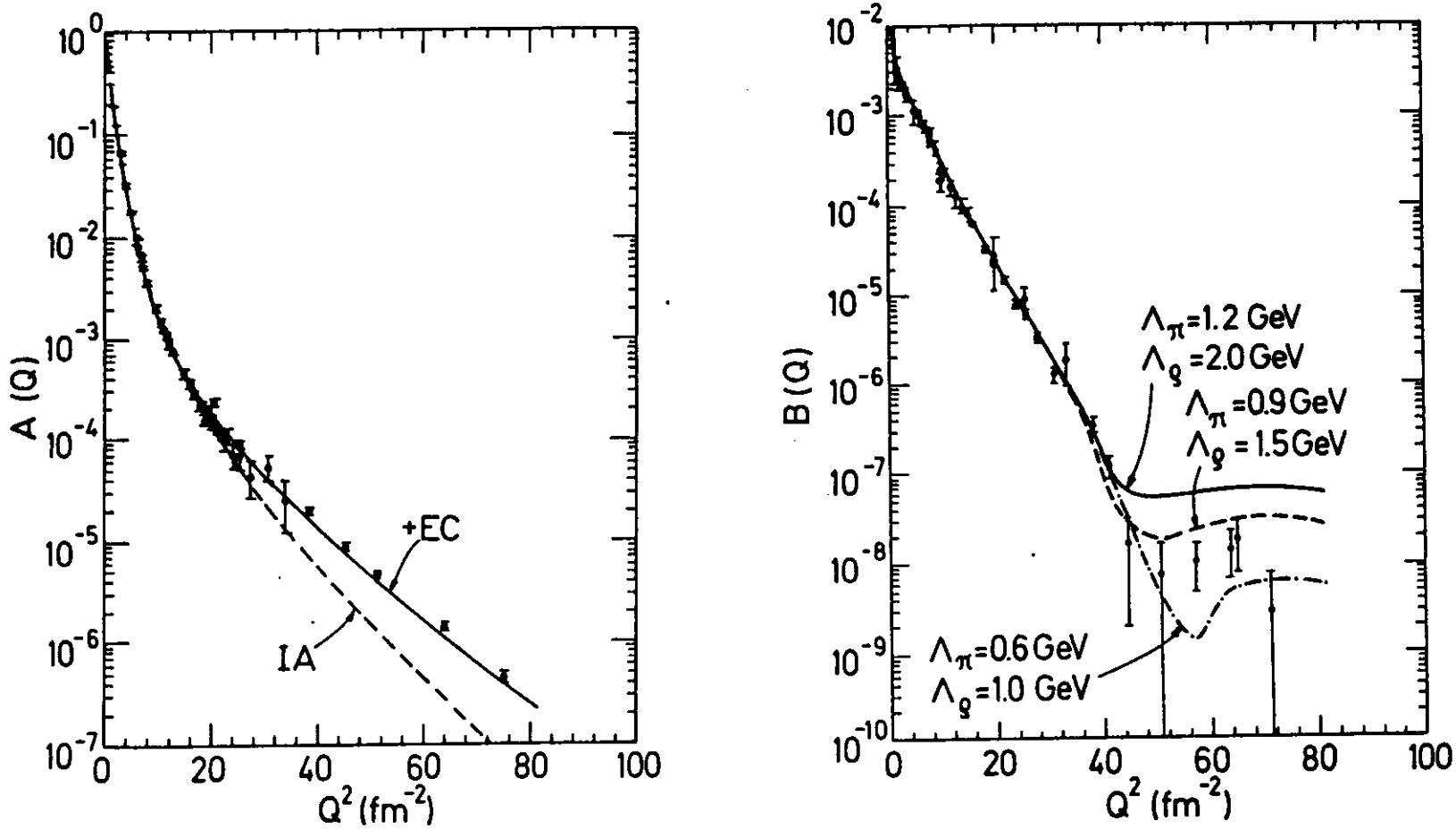
A (Q)
B (Q)
Q² (fm⁻²)
+EC
IA
Λπ=1.2 GeV
Λρ=2.0 GeV
Λπ=0.9 GeV
Λρ=1.5 GeV
Λπ=0.6 GeV
Λρ=1.0 GeV

FIGURE 6

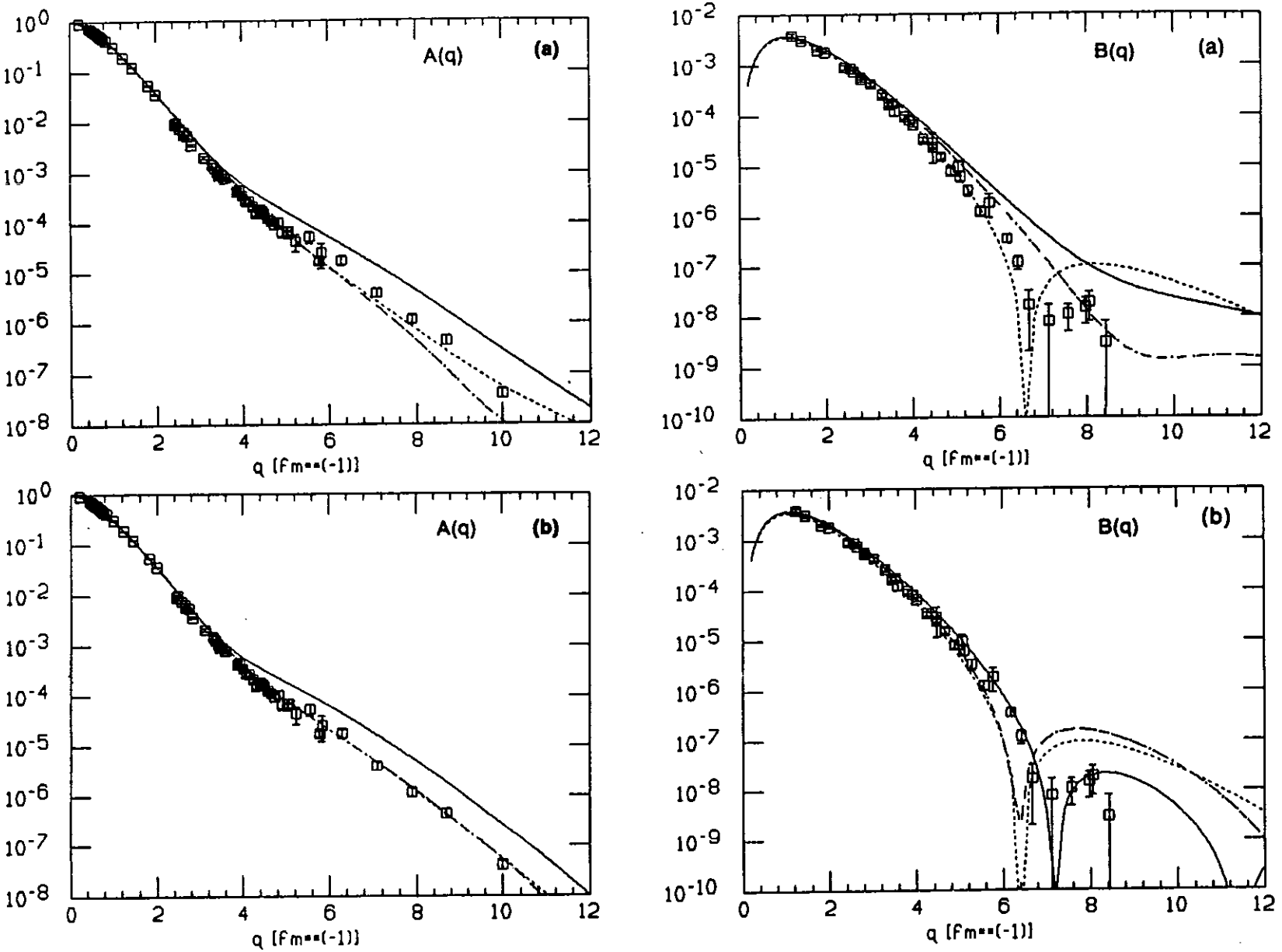

FIGURE 7

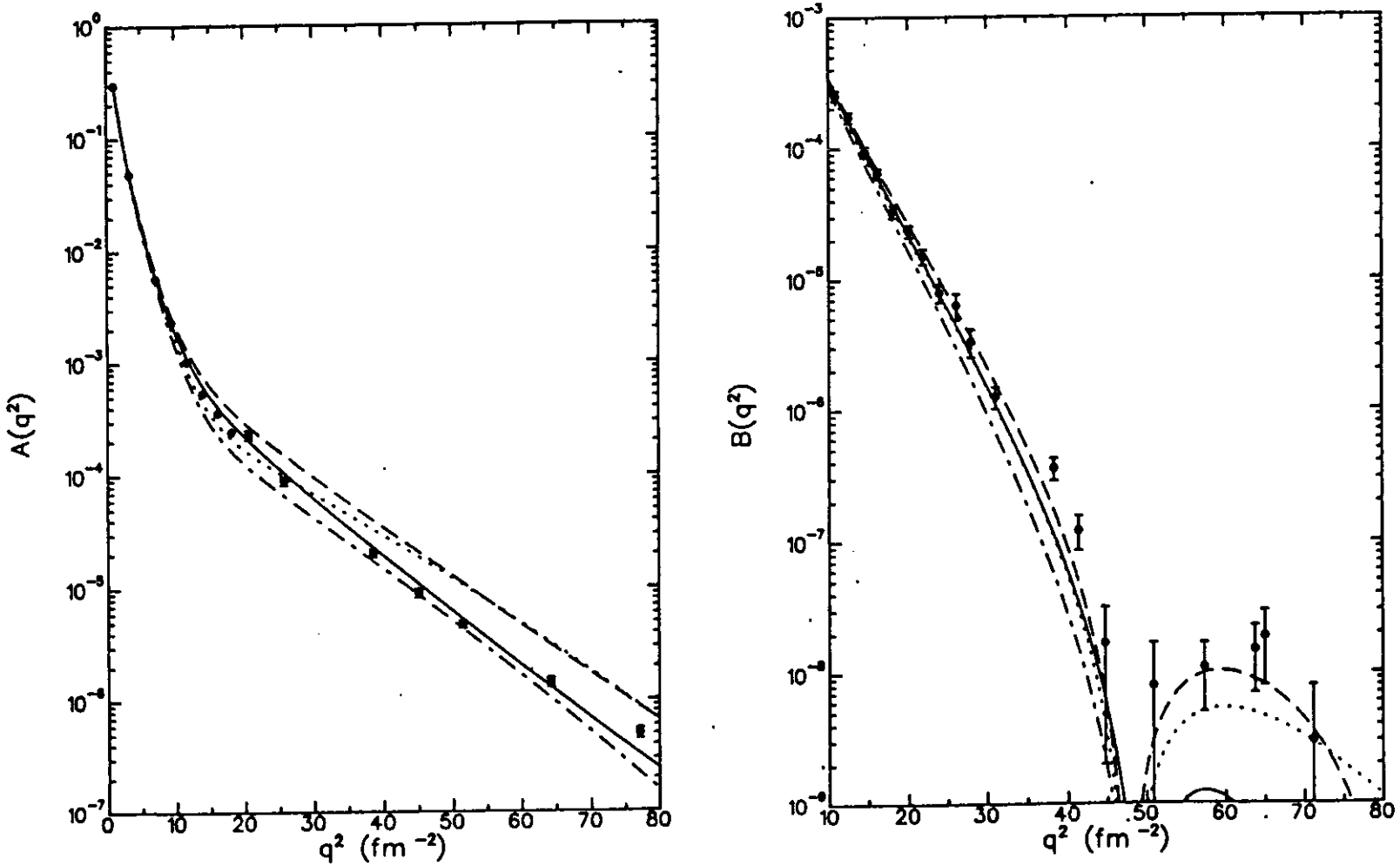

FIGURE 9

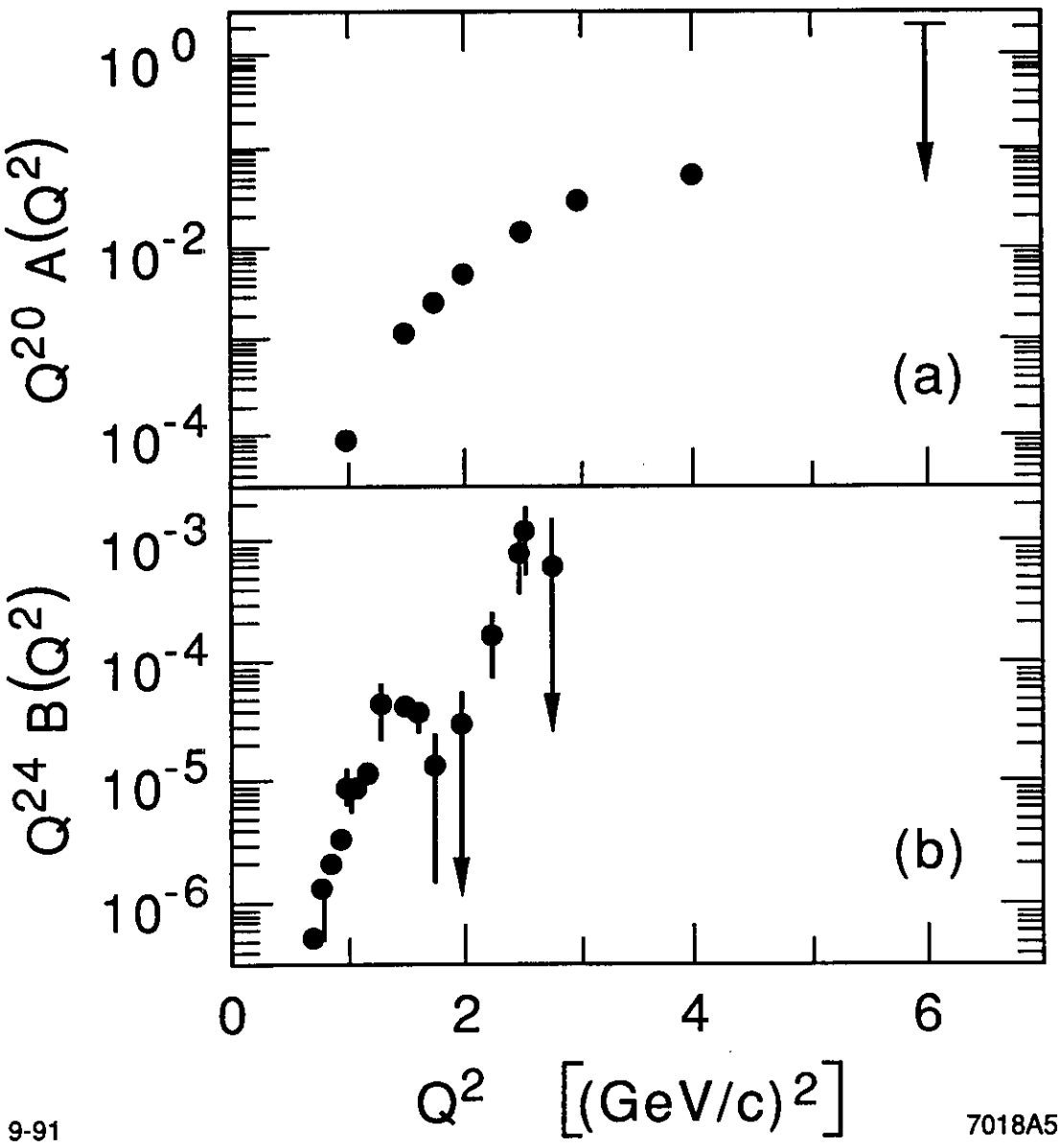
10^0
10^{-2}
10^{-4}
$Q^{20}\,A(Q^2)$
(a)
10^{-3}
10^{-4}
10^{-5}
10^{-6}
$Q^{24}\,B(Q^2)$
(b)
0
2
4
6
Q^2 $[(GeV/c)^2]$
9-91
7018A5

FIGURE 10

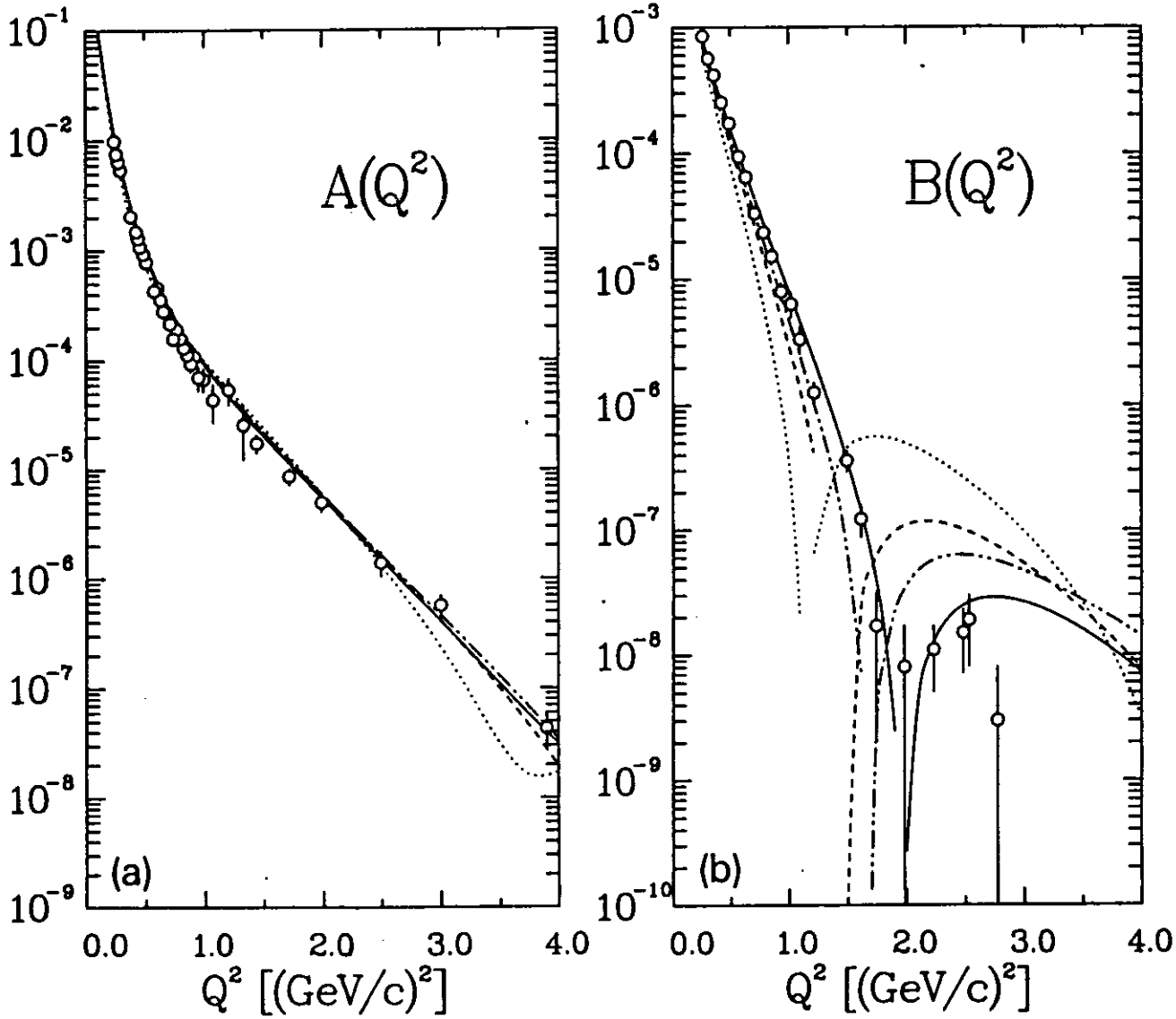

FIGURE 8

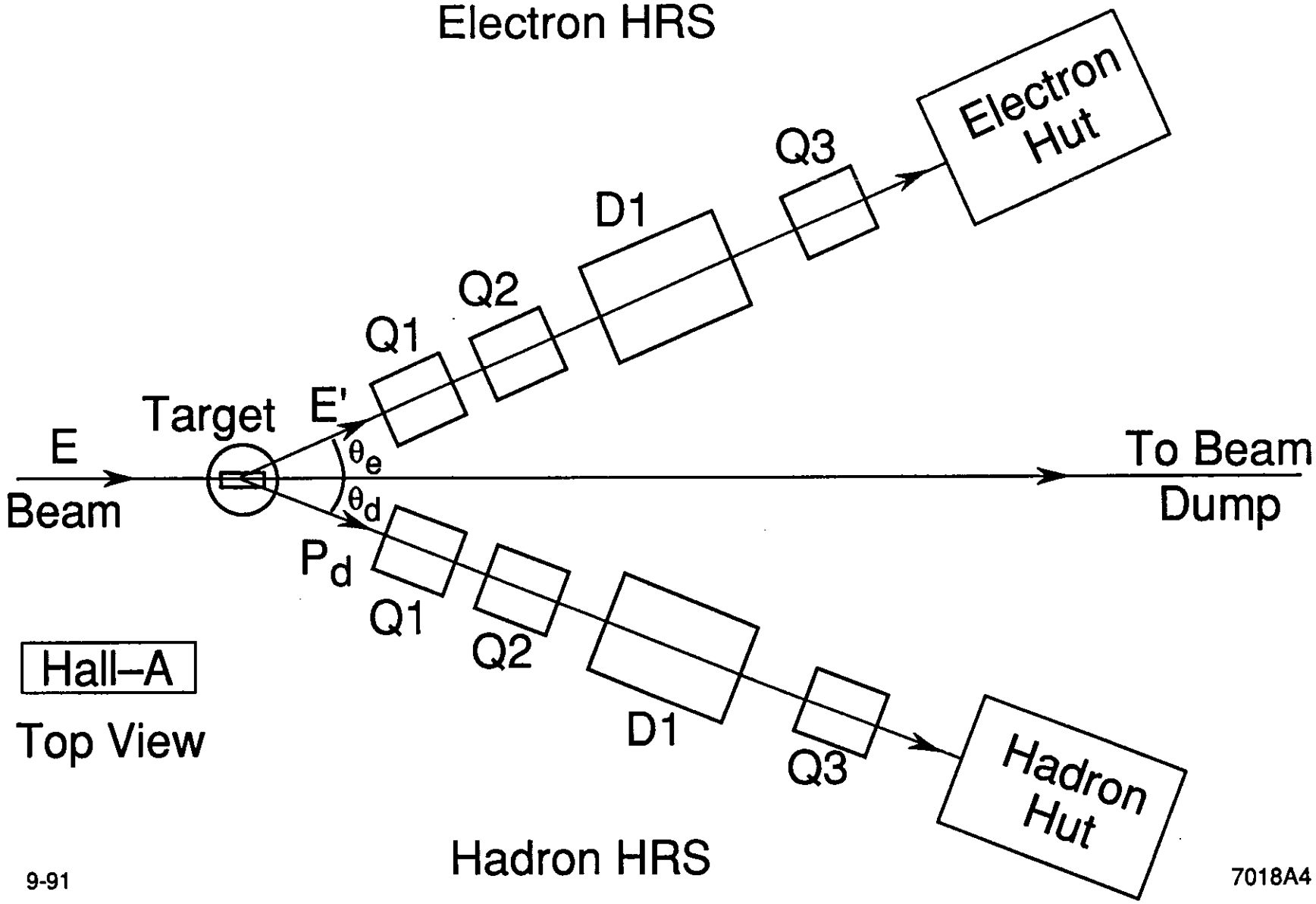
Electron HRS
Electron Hut
Q3
D1
Q2
Q1
E'
Target
E
Beam
θ_e
θ_d
To Beam Dump
P_d
Q1
Q2
D1
Q3
Hadron Hut
Hall–A
Top View
Hadron HRS
9-91
7018A4

FIGURE 11

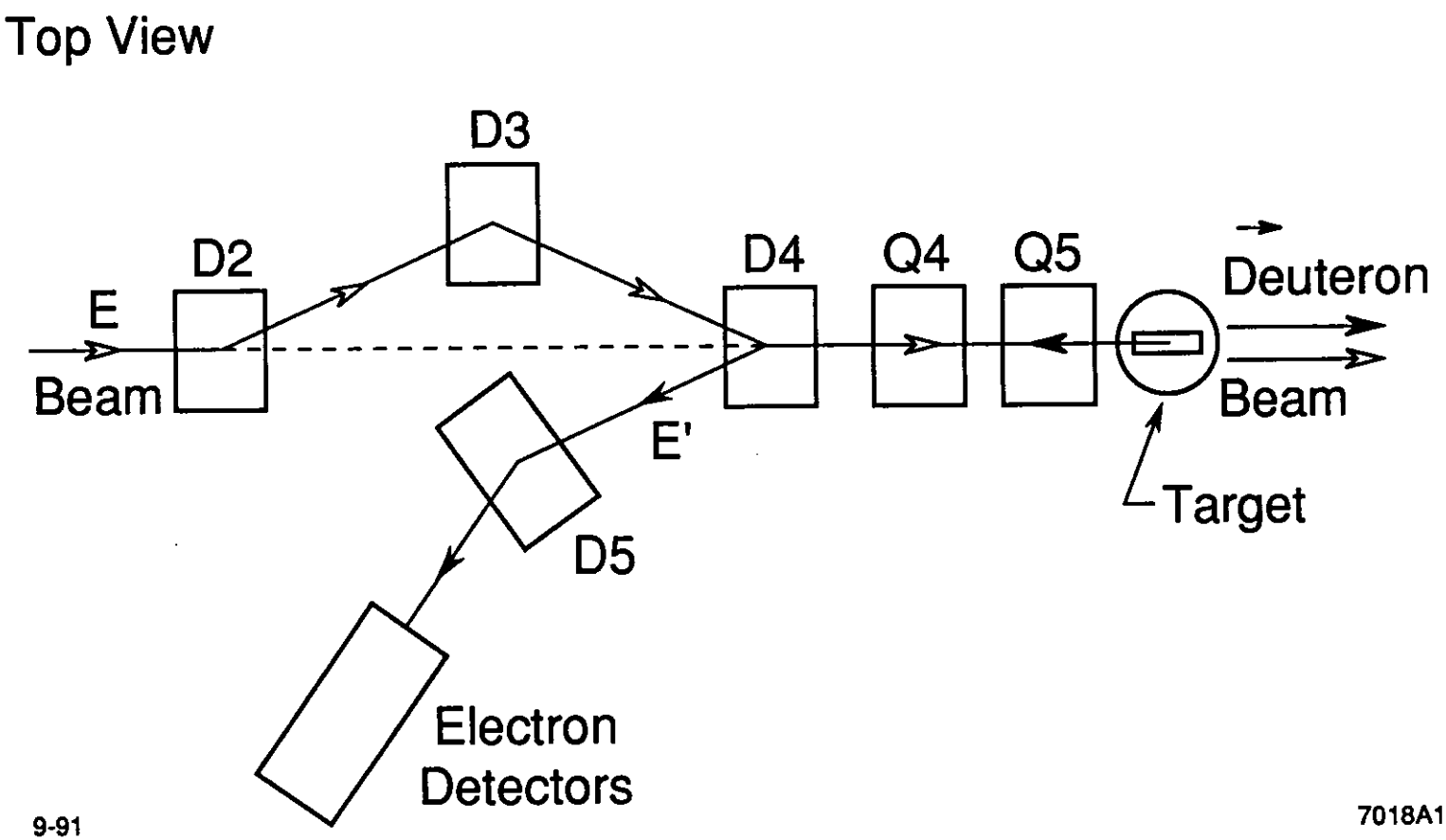
Top View
D3
D2
E
Beam
D4
Q4
Q5
Deuteron
Beam
E'
Target
D5
Electron
Detectors
9-91
7018A1

FIGURE 12

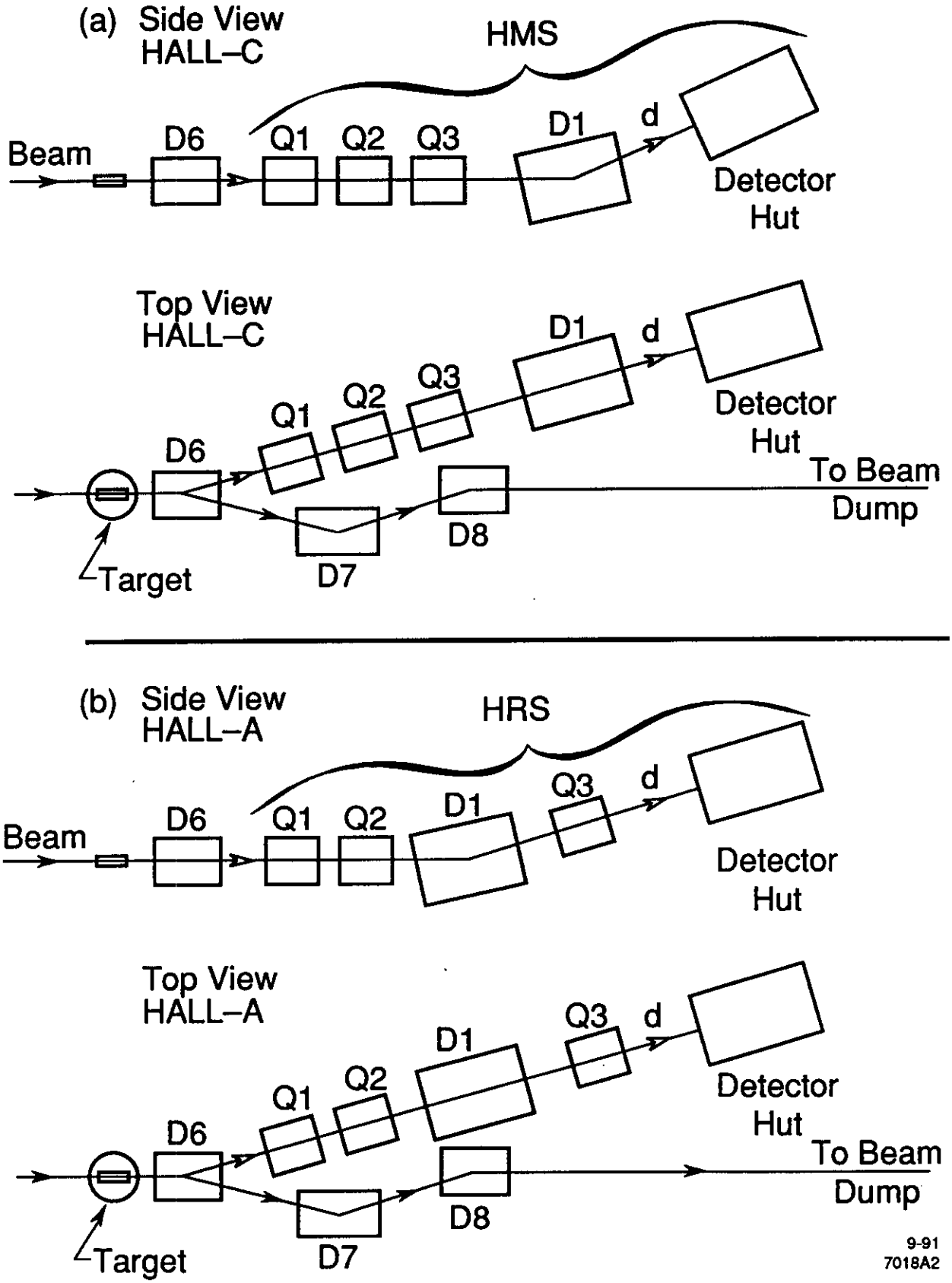
(a) Side View
HALL–C
HMS
Beam
D6
Q1
Q2
Q3
D1
d
Detector
Hut
Top View
HALL–C
D1
d
Q3
Q2
Q1
D6
Detector
Hut
To Beam
Dump
D8
Target
D7
(b) Side View
HALL–A
HRS
Beam
D6
Q1
Q2
D1
Q3
d
Detector
Hut
Top View
HALL–A
Q3
d
D1
Q2
Q1
D6
Detector
Hut
To Beam
Dump
D8
Target
D7
9-91
7018A2

FIGURE 13

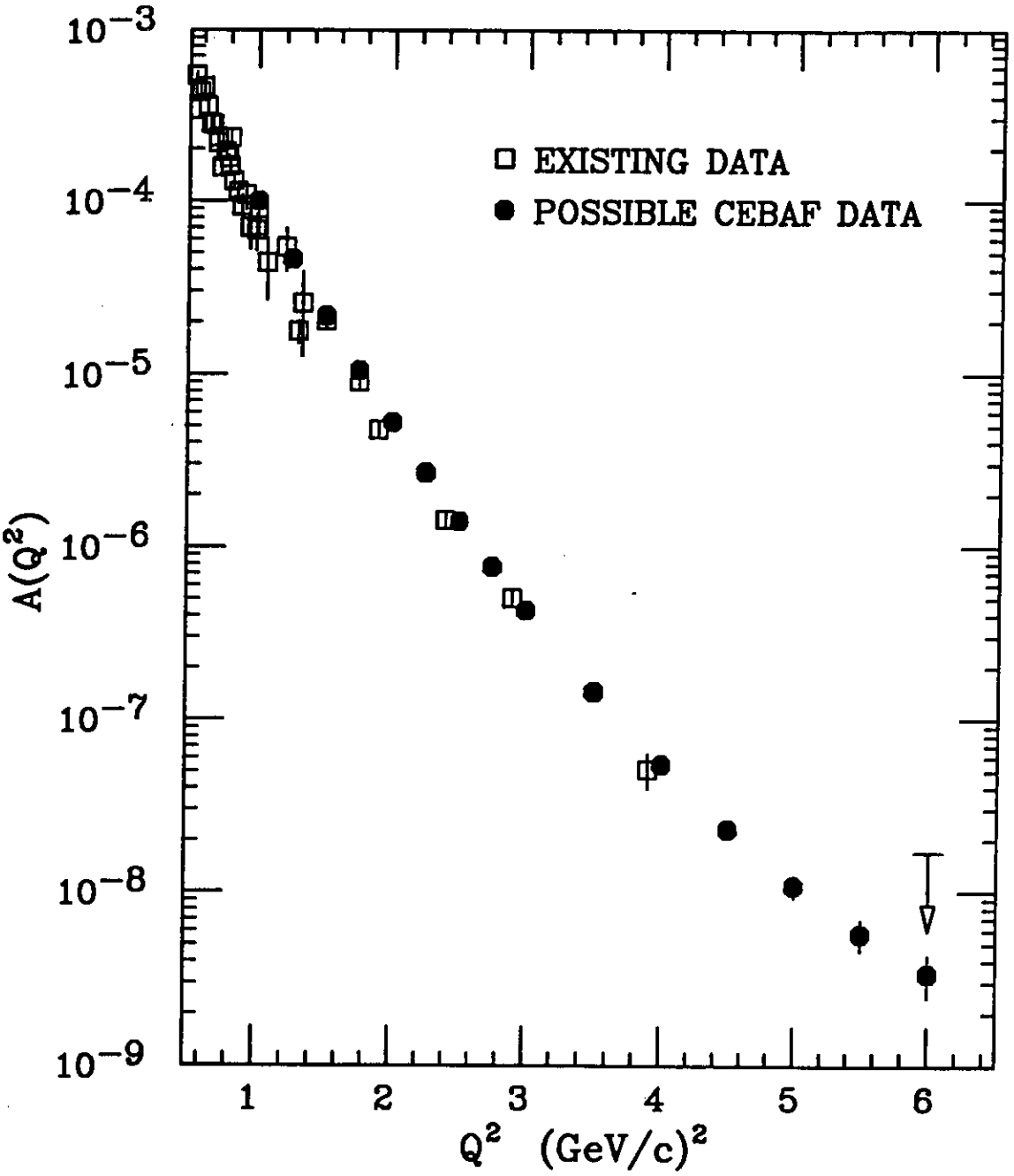
EXISTING DATA
POSSIBLE CEBAF DATA
10^{-3}
10^{-4}
10^{-5}
10^{-6}
10^{-7}
10^{-8}
10^{-9}
$A(Q^2)$
1
2
3
4
5
6
Q^2 $(GeV/c)^2$

FIGURE 14

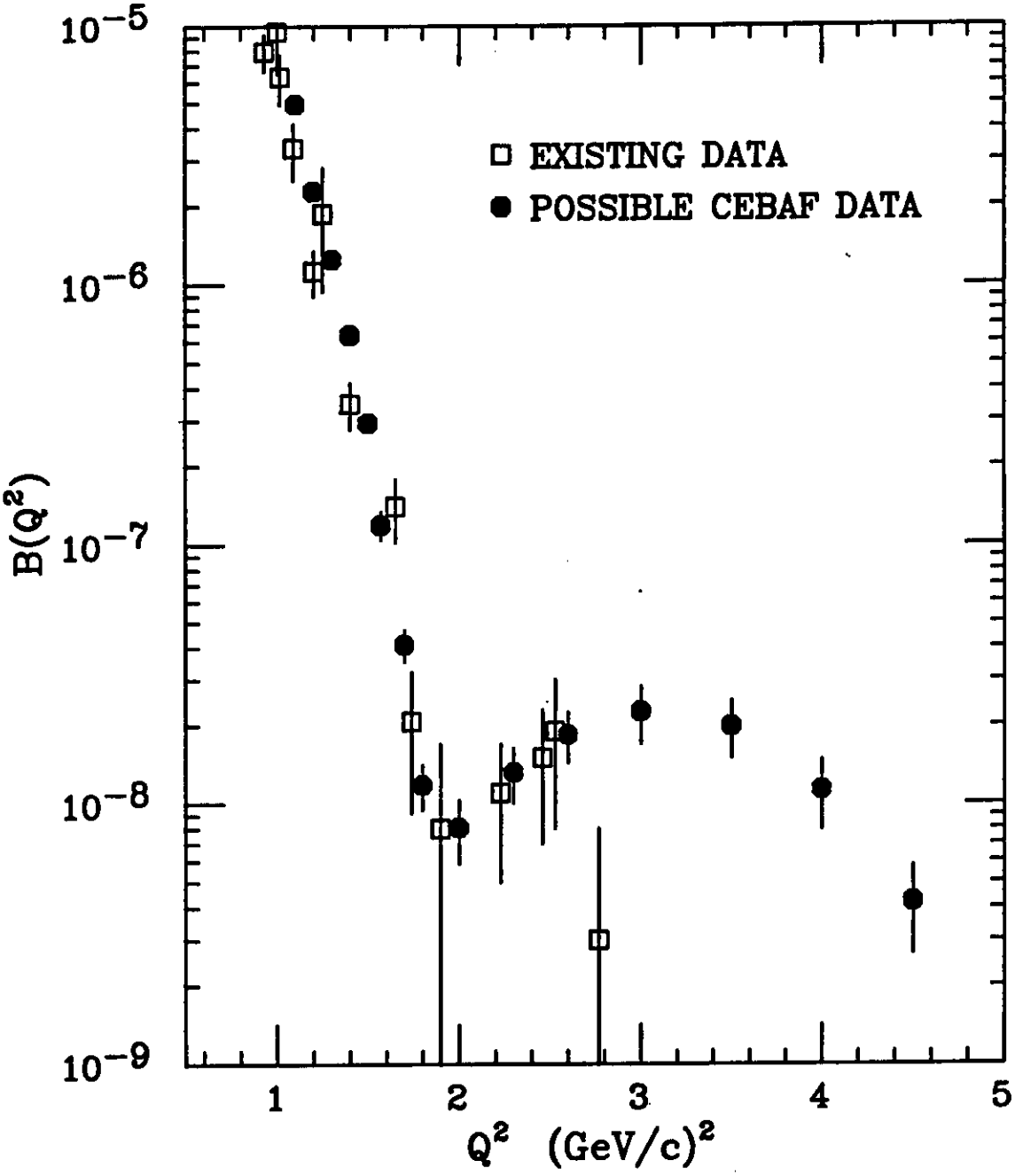
EXISTING DATA
POSSIBLE CEBAF DATA
$B(Q^2)$
10^{-5}
10^{-6}
10^{-7}
10^{-8}
10^{-9}
1
2
3
4
5
Q^2 $(GeV/c)^2$

FIGURE 15

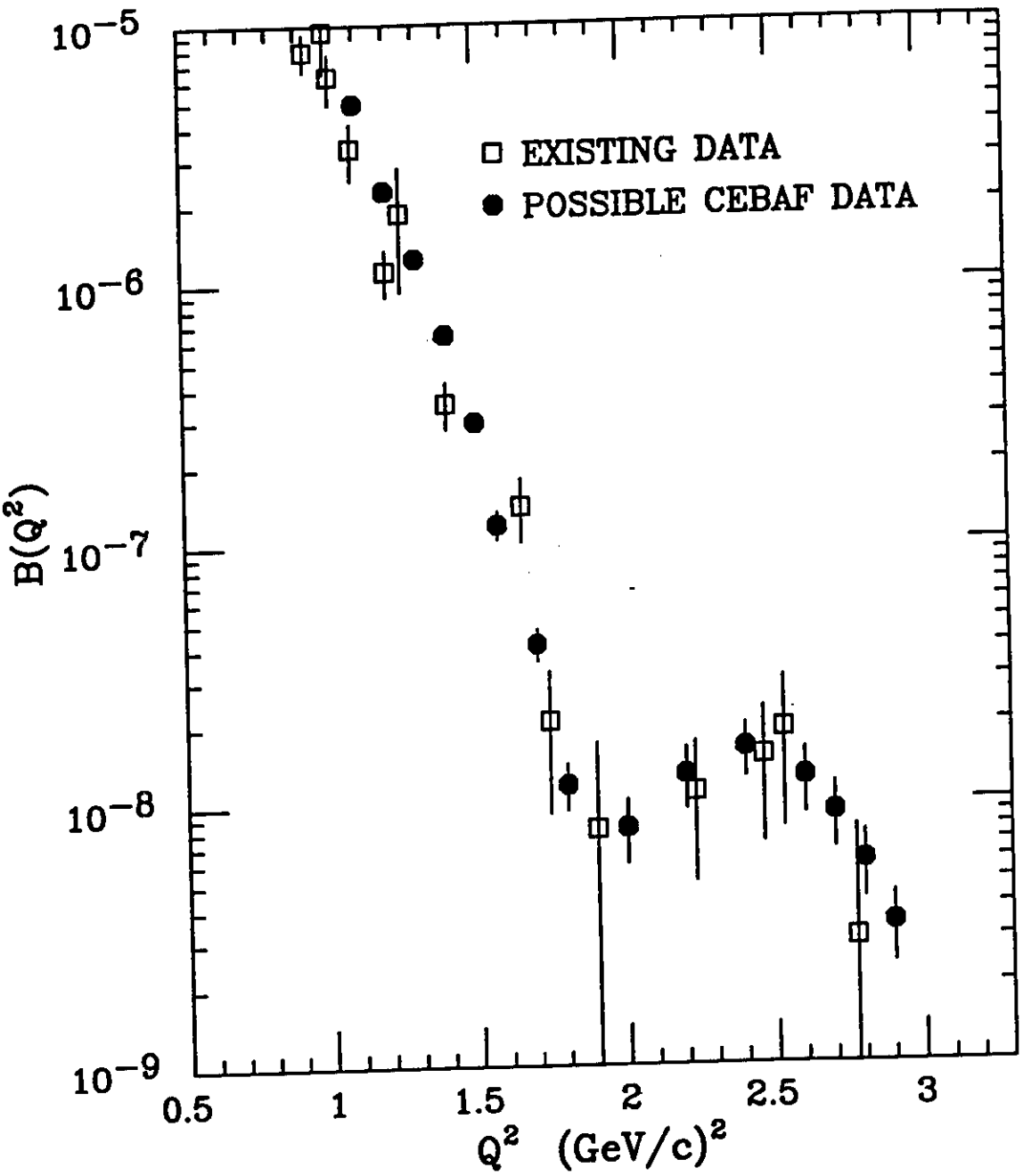
EXISTING DATA
POSSIBLE CEBAF DATA
$B(Q^2)$
10^{-5}
10^{-6}
10^{-7}
10^{-8}
10^{-9}
0.5
1
1.5
2
2.5
3
Q^2 $(GeV/c)^2$

FIGURE 16

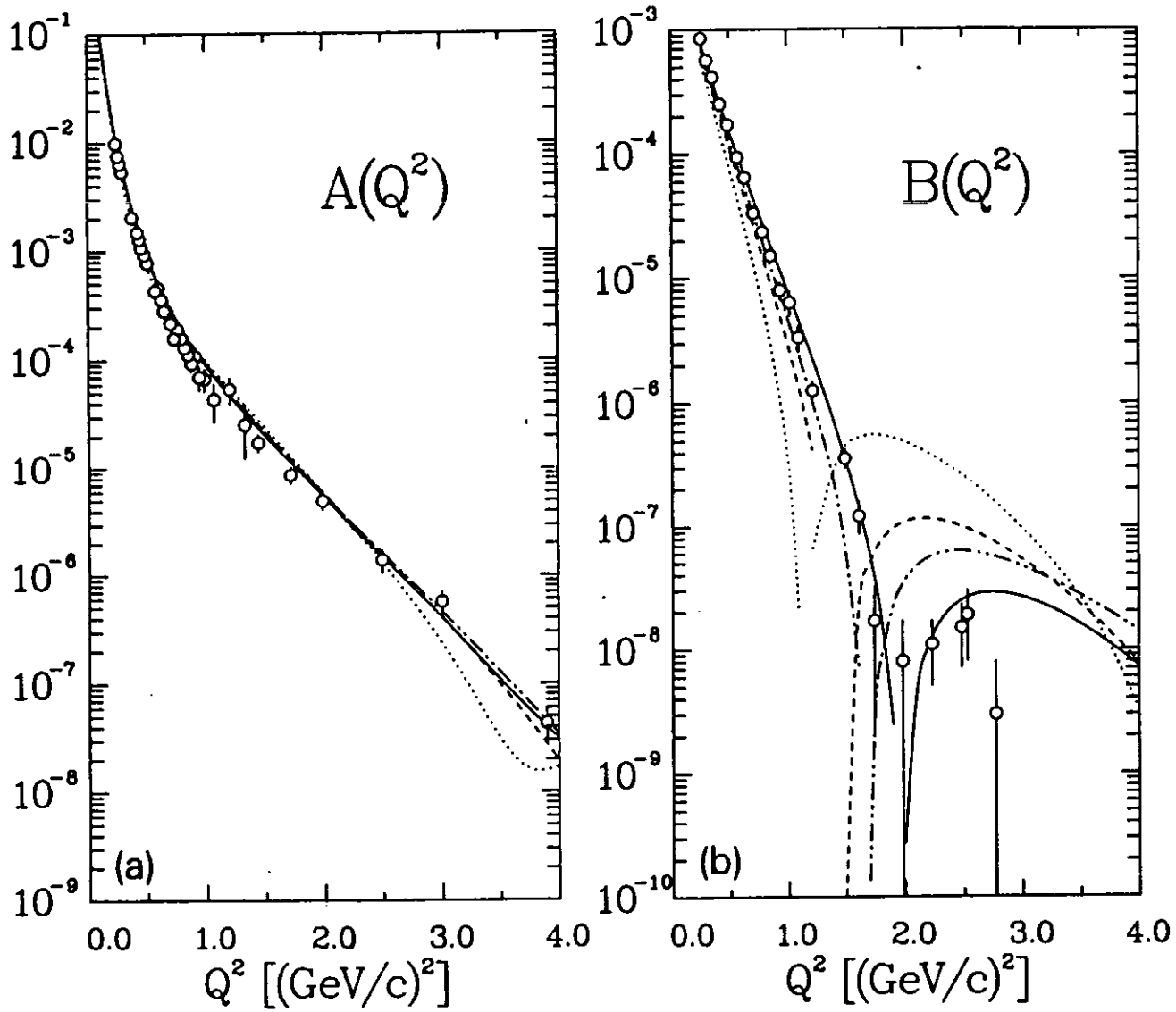

FIGURE 8

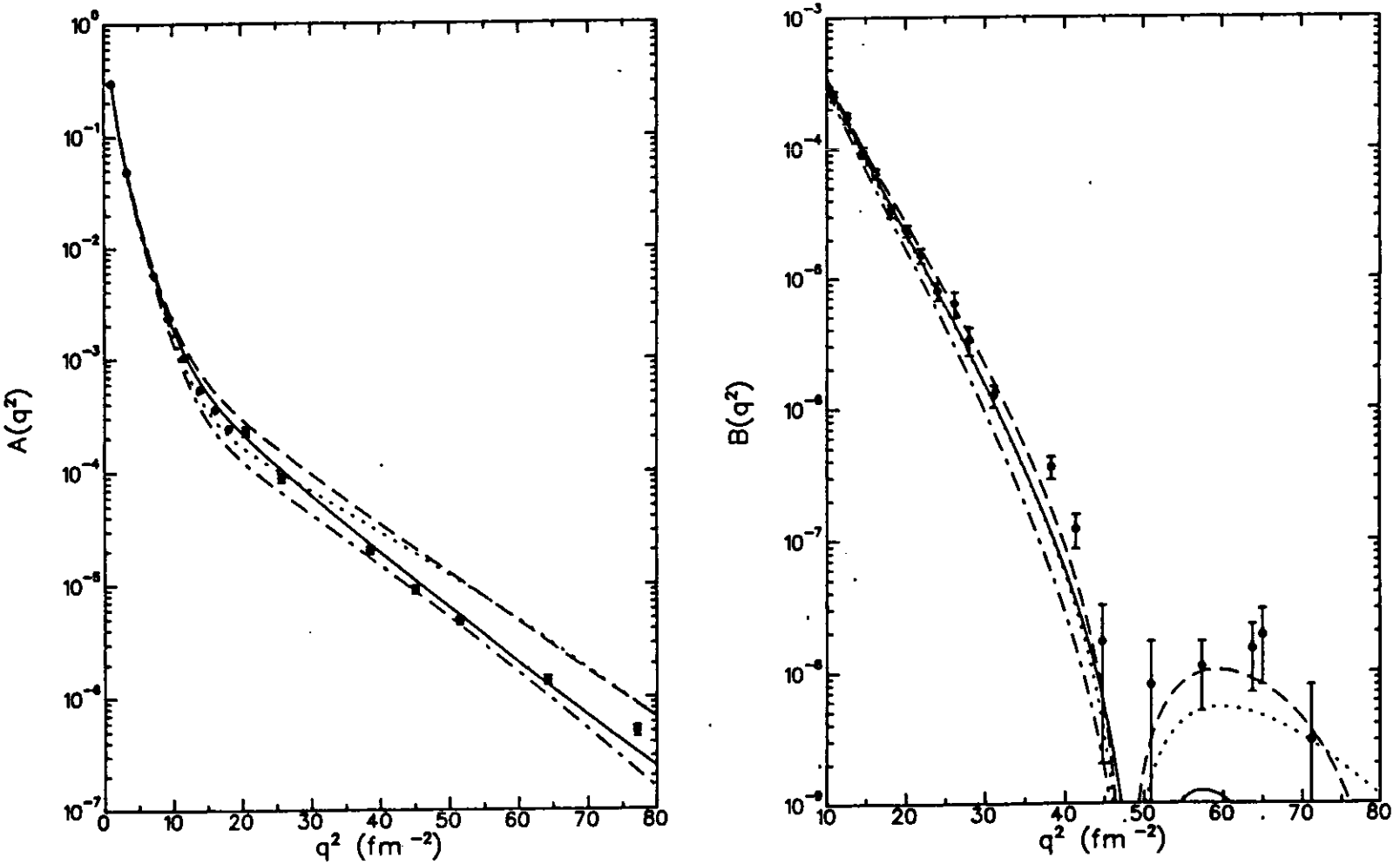

FIGURE 9

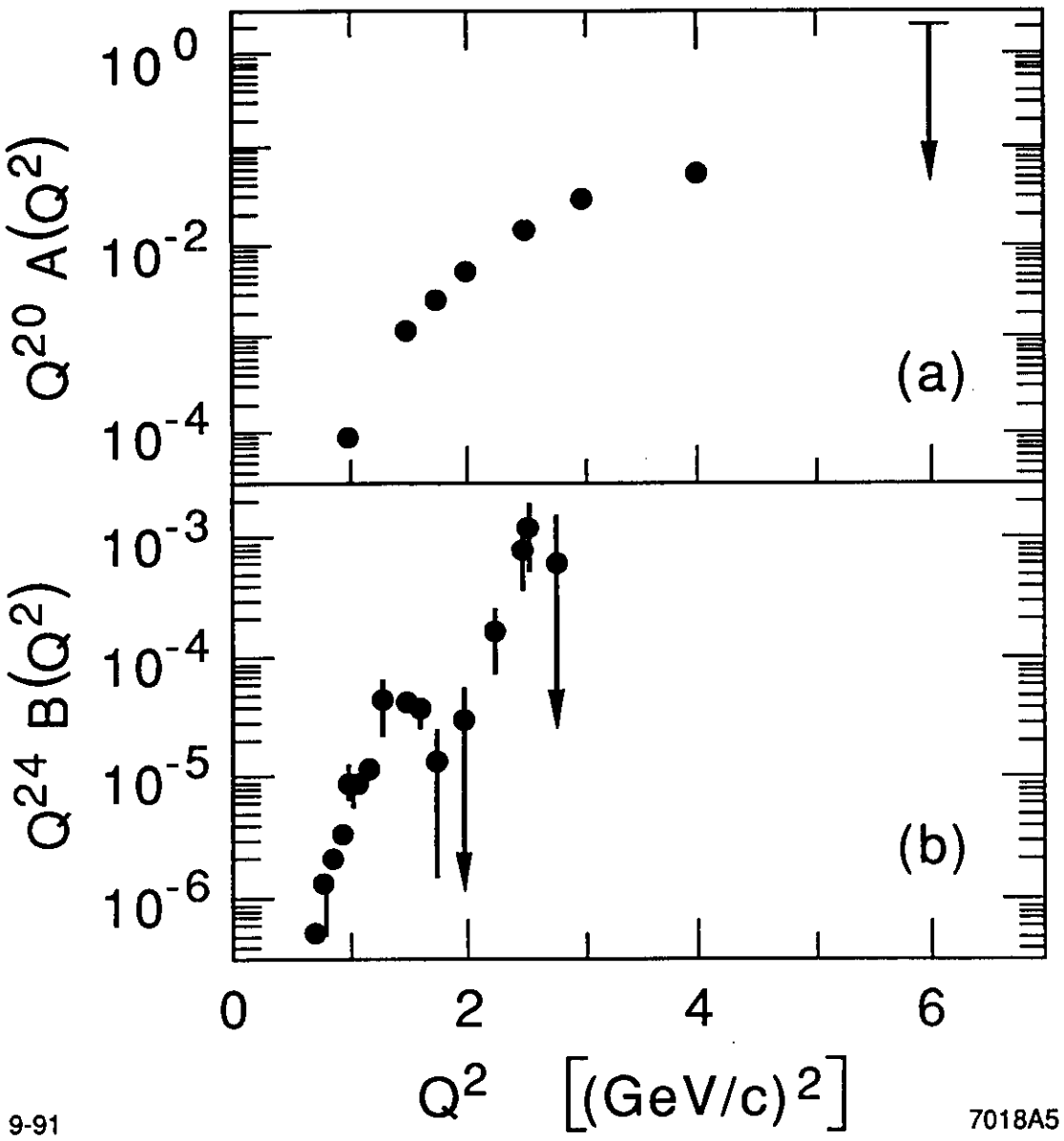
10^0
10^{-2}
10^{-4}
$Q^{20}\,A(Q^2)$
(a)
10^{-3}
10^{-4}
10^{-5}
10^{-6}
$Q^{24}\,B(Q^2)$
(b)
0
2
4
6
Q^2 $[(GeV/c)^2]$
9-91
7018A5

FIGURE 10

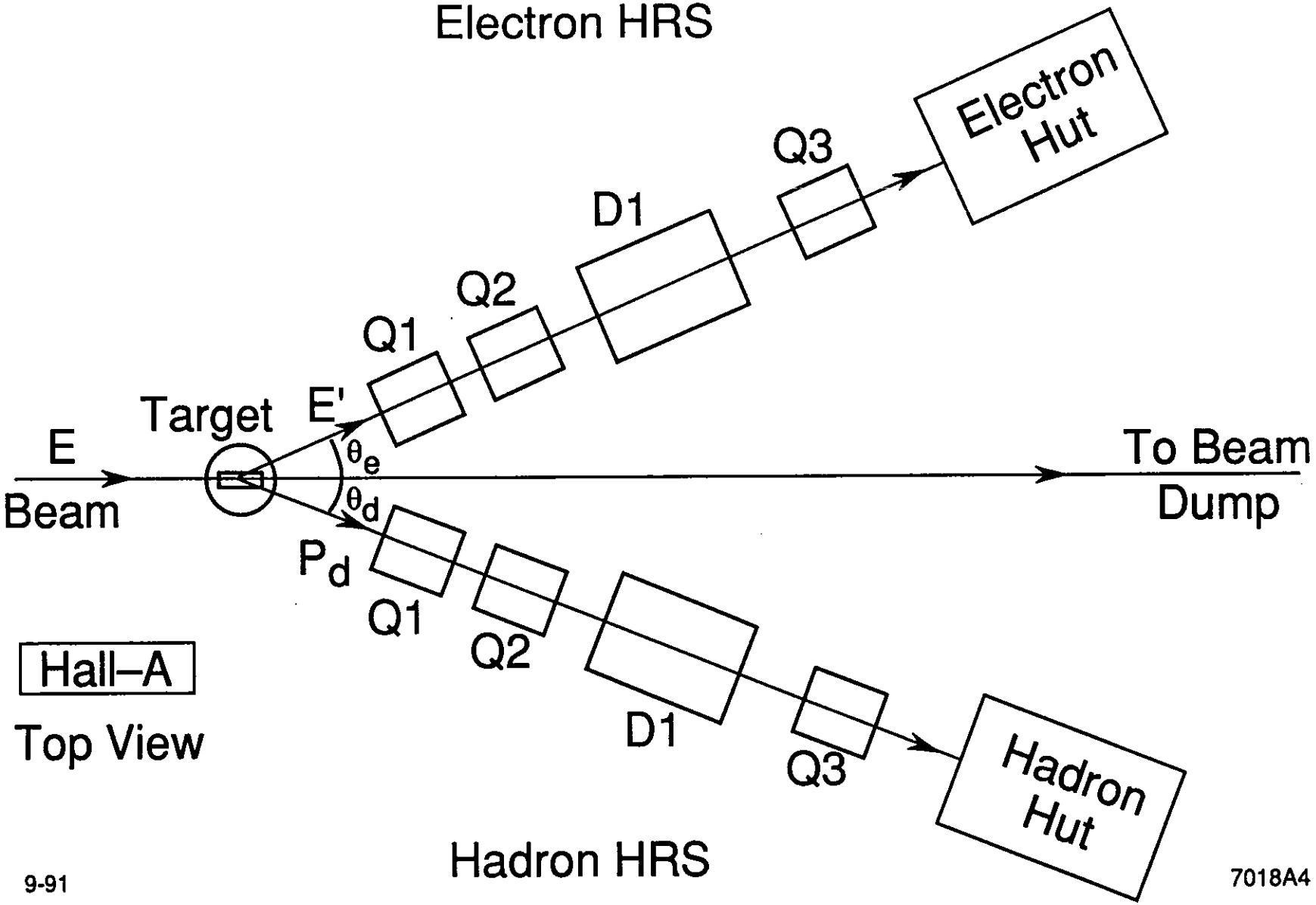
Electron HRS
Electron Hut
Q3
D1
Q2
Q1
E'
Target
E
Beam
θe
θd
To Beam Dump
Pd
Q1
Q2
D1
Q3
Hadron Hut
Hall–A
Top View
Hadron HRS
9-91
7018A4

FIGURE 11

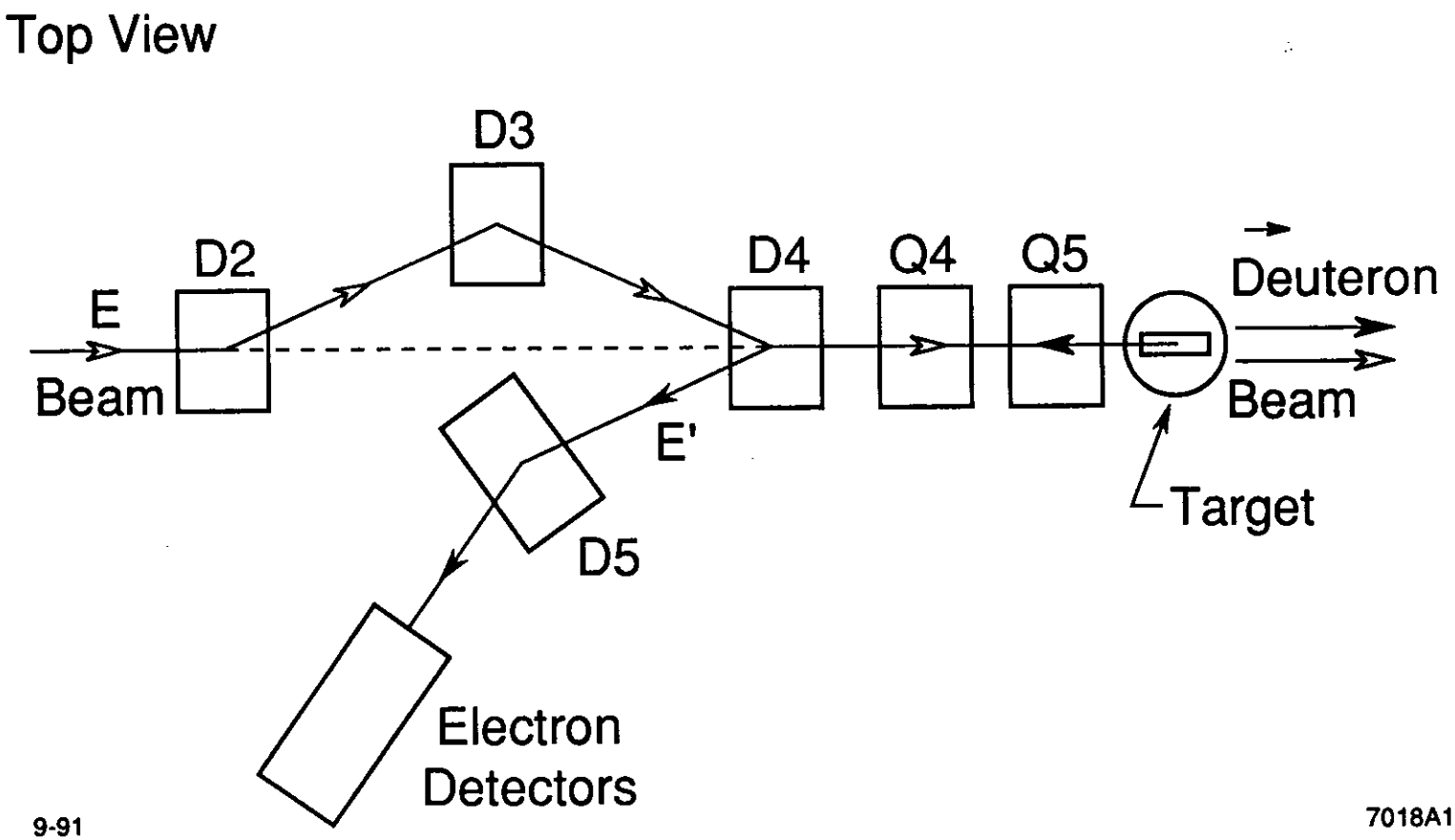
Top View
D3
D2
E
Beam
D4
Q4
Q5
Deuteron
Beam
E'
Target
D5
Electron
Detectors
9-91
7018A1

FIGURE 12

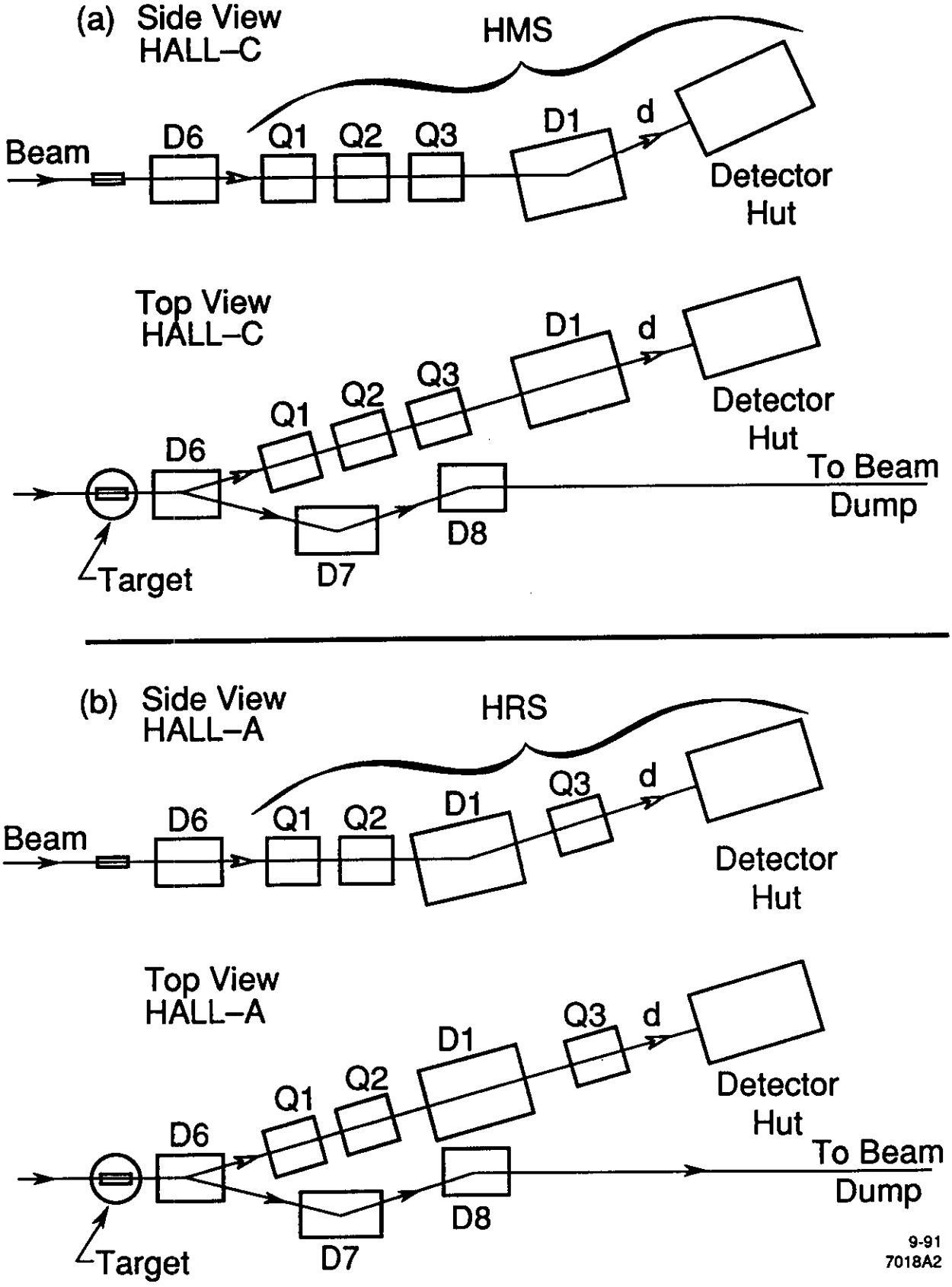
(a) Side View
HALL–C
HMS
Beam
D6
Q1
Q2
Q3
D1
d
Detector
Hut
Top View
HALL–C
D1
d
Q3
Q2
Q1
D6
Detector
Hut
To Beam
Dump
D8
D7
Target
(b) Side View
HALL–A
HRS
Beam
D6
Q1
Q2
D1
Q3
d
Detector
Hut
Top View
HALL–A
Q3
d
D1
Q2
Q1
D6
Detector
Hut
To Beam
Dump
D8
D7
Target
9-91
7018A2

FIGURE 13

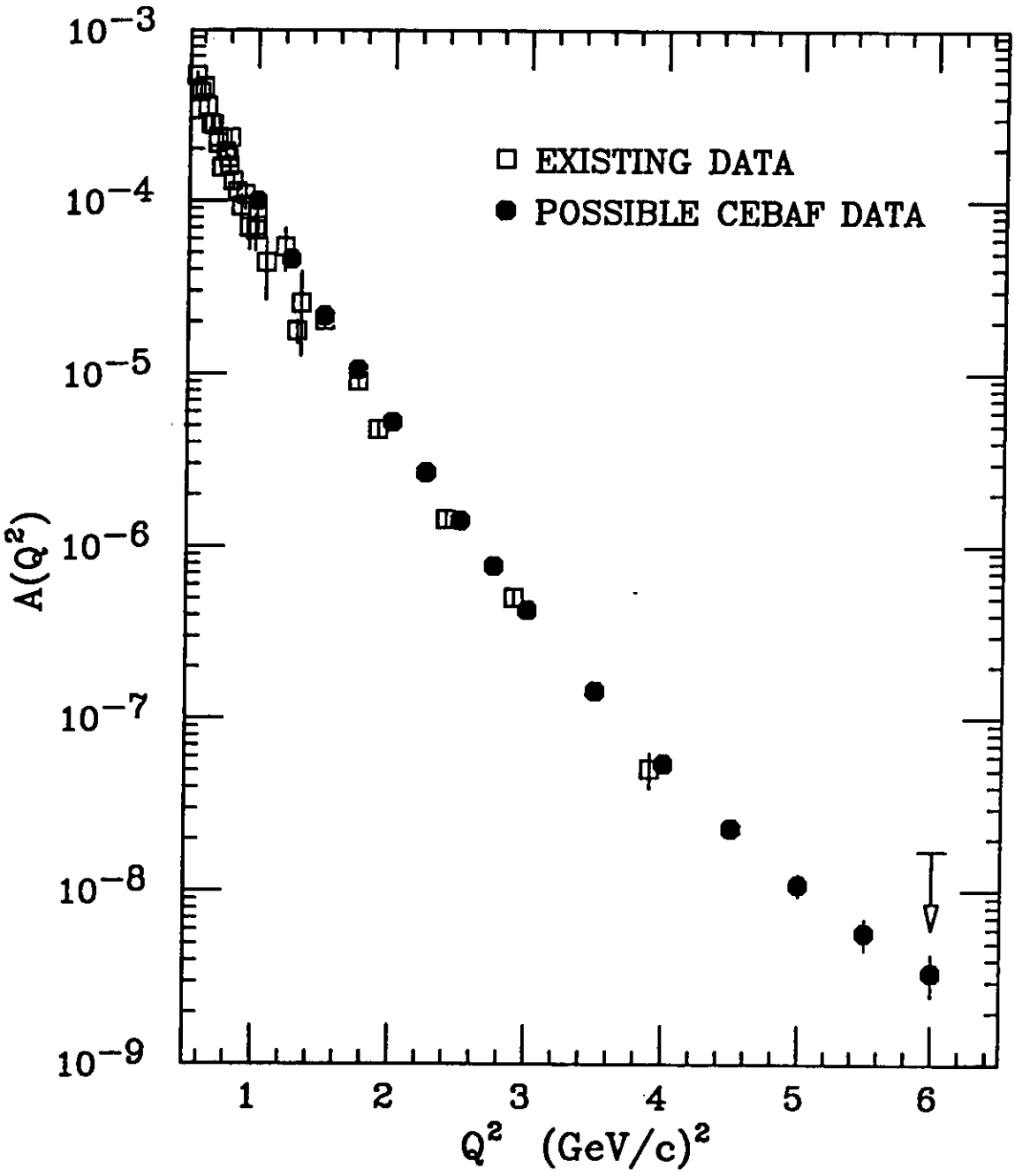
EXISTING DATA
POSSIBLE CEBAF DATA
10^{-3}
10^{-4}
10^{-5}
10^{-6}
10^{-7}
10^{-8}
10^{-9}
$A(Q^2)$
1
2
3
4
5
6
Q^2 $(GeV/c)^2$

FIGURE 14

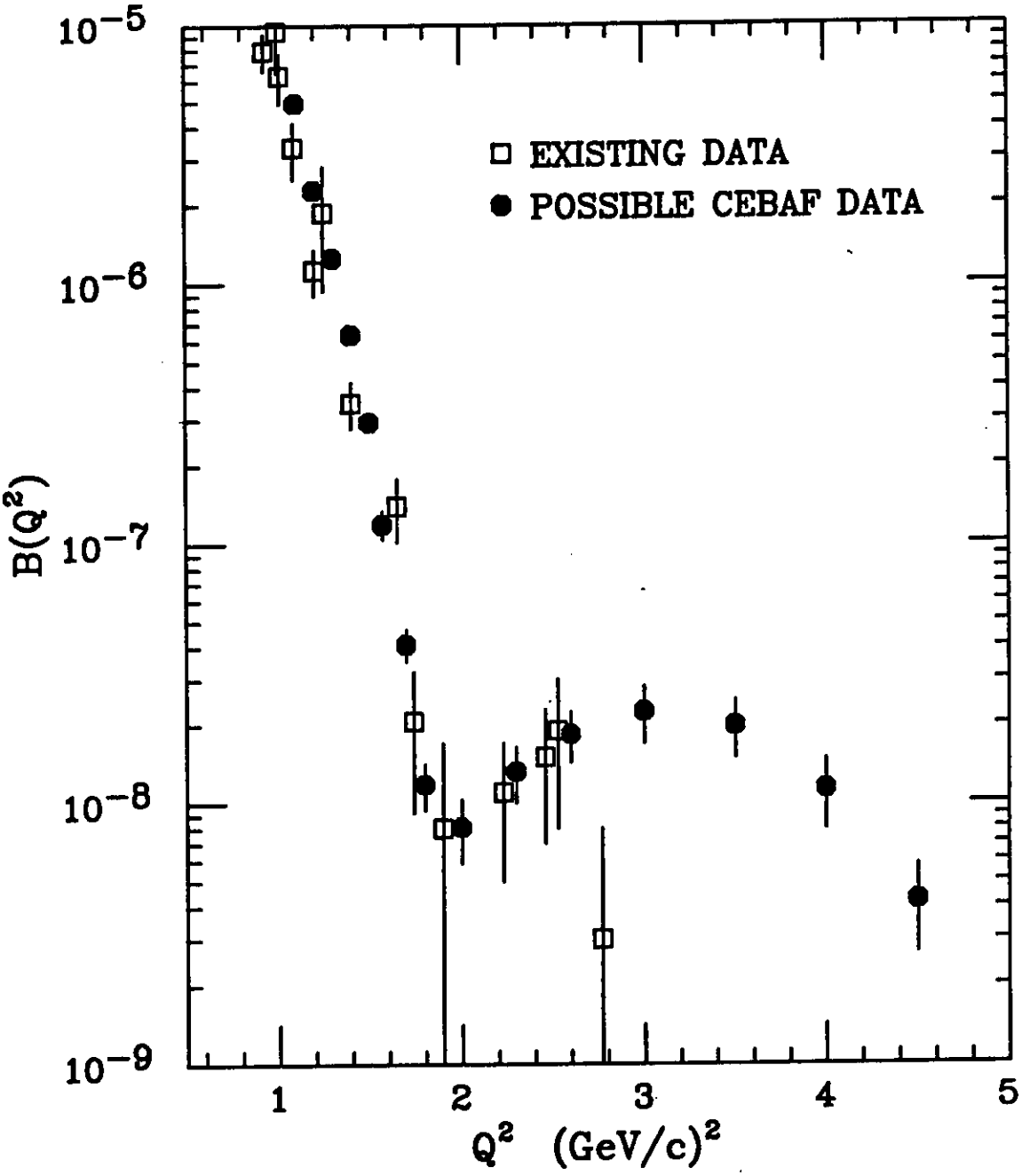
10^{-5}
10^{-6}
10^{-7}
10^{-8}
10^{-9}
$B(Q^2)$
EXISTING DATA
POSSIBLE CEBAF DATA
1
2
3
4
5
Q^2 $(GeV/c)^2$

FIGURE 15

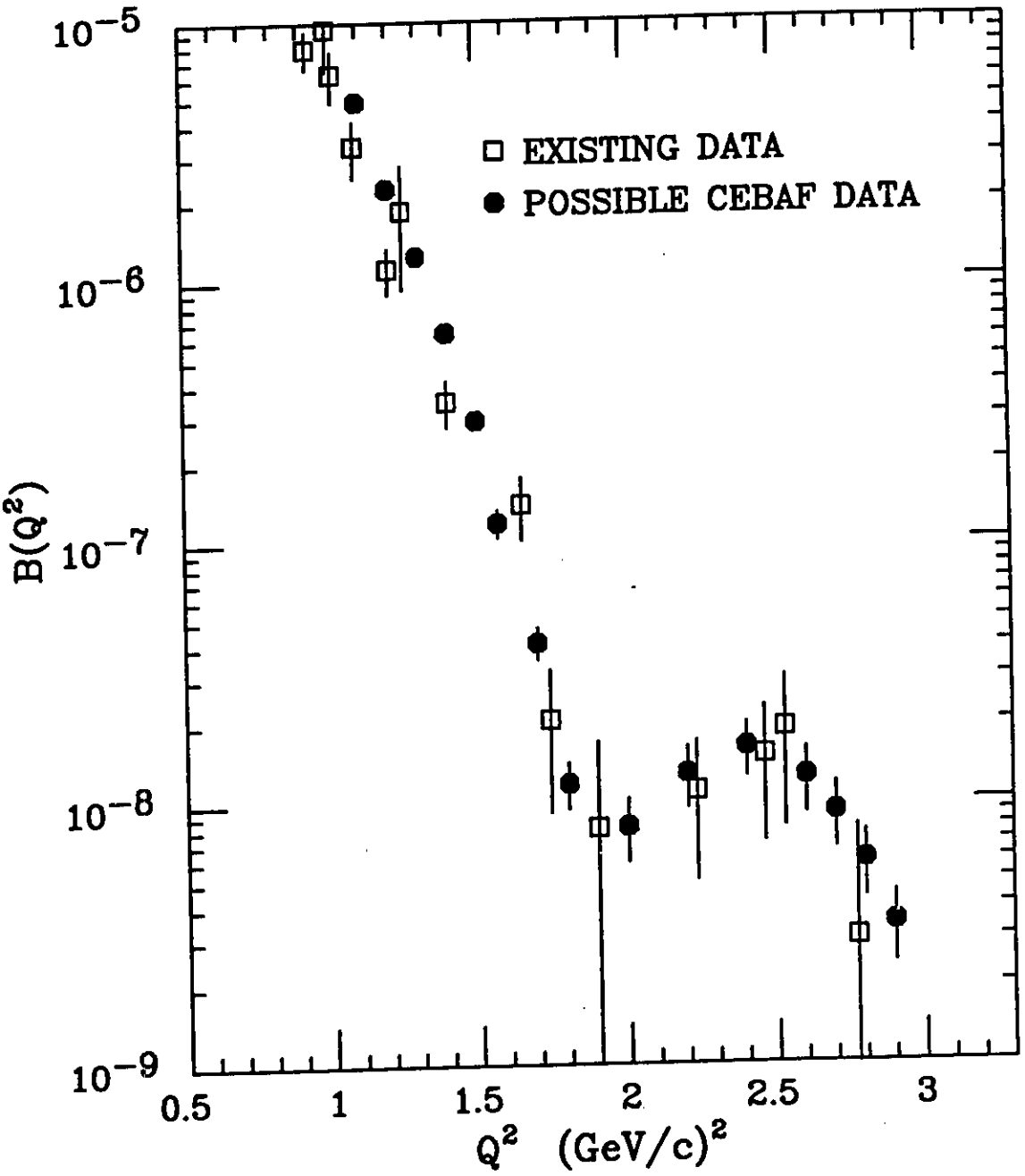
EXISTING DATA
POSSIBLE CEBAF DATA
$B(Q^2)$
10^{-5}
10^{-6}
10^{-7}
10^{-8}
10^{-9}
0.5
1
1.5
2
2.5
3
Q^2 $(GeV/c)^2$

FIGURE 16